

ORIGINAL RESEARCH ARTICLE

Novel 1,3-dioxolane–coumarin hybrids: From synthesis to pharmacological *In Vitro-In Silico* profiling

Duha Adnan Hassan, Yasser Fakri Mustafa*

Department of Pharmaceutical Chemistry, College of Pharmacy, University of Mosul, Mosul, 41001, Iraq

*Corresponding author: Yasser Fakri Mustafa, Dr.yassermustafa@uomosul.edu.iq

ABSTRACT

In this study, we report the design, synthesis, and comprehensive biological evaluation of a novel series of linear 1,3-dioxolane–coumarin hybrids (**DCH1–DCH7**) as promising multi-target therapeutic agents. The synthesis involved an optimized multi-step approach beginning with a Pechmann condensation followed by selective esterification reactions, yielding high-purity compounds confirmed via FTIR, ¹H-NMR, and ¹³C-NMR analyses. The hybrids were systematically screened for their antioxidant, anticancer, anti-inflammatory, antidiabetic, and antimicrobial activities. In addition, their biocompatibility was assessed using non-cancerous human cell lines and commensal bacterial strains. Among the synthesized hybrids, **DCH4** exhibited remarkable antioxidant and anticancer properties, while **DCH1** showed superior anti-inflammatory and antifungal activity. **DCH2** demonstrated potent antidiabetic and anti-anaerobic bacterial efficacy, and **DCH5** emerged as the most active against aerobic gram-negative bacteria. These bioactivities were closely linked to specific structural modifications, as revealed through structure–activity relationship analyses. *In silico* evaluations using ProTox-II, PreADME, and SwissADME tools predicted favorable drug-likeness, low toxicity, high oral bioavailability, and acceptable pharmacokinetic profiles, further supporting their therapeutic relevance. Importantly, all hybrids displayed minimal cytotoxic effects on non-cancerous cells and exhibited selective antimicrobial actions, sparing beneficial gut microbiota. This highlights their potential as safer alternatives to conventional therapies. The introduction of the 1,3-dioxolane moiety into the coumarin scaffold contributed significantly to the observed bioactivities, suggesting this hybrid framework as a versatile platform for future drug development. Overall, our findings establish these 1,3-dioxolane–coumarin hybrids as promising multifunctional drug candidates with broad-spectrum pharmacological potential and a strong safety profile, warranting further investigation and development.

Keywords: hybridization; 1,3-dioxolane; biosafety; coumarin; drug-likeness; multi-target therapeutics

ARTICLE INFO

Received: 1 April 2025
Accepted: 27 April 2025
Available online: 30 April 2025

COPYRIGHT

Copyright © 2025 by author(s).
Applied Chemical Engineering is published by
Arts and Science Press Pte. Ltd. This work is
licensed under the Creative Commons
Attribution-NonCommercial 4.0 International
License (CC BY 4.0).
<https://creativecommons.org/licenses/by/4.0/>

1. Introduction

Coumarins (COMs) represent a diverse group of phenolic compounds naturally occurring in plants, characterized by a fused benzene and α -pyrone ring system^[1,2]. More than 1,300 structural variants have been identified, primarily functioning as secondary metabolites in plants, fungi, and bacteria^[3–5]. Due to their abundance in medicinal plants and relatively low toxicity, COMs have garnered significant attention for their clinical and biochemical properties^[6–8]. The study of COMs is fascinating due to their low molecular weight, simple structure, and extensive electron conjugation system. They also offer good solubility, along with excellent bioavailability, biosafety, and compatibility^[9,10]. These compounds exhibit strong therapeutic potential and play a vital role in modern healthcare due to their diverse pharmacological and biological activities, making them essential in medicine^[11–13]. These medicinal activities include anticancer^[14–16],

anti-inflammatory^[17], anticoagulant^[18,19], antihypertensive^[20,21], anticonvulsant^[22-24], antioxidant^[25-27], antimicrobial^[28-30], antidiabetic^[31-33], and neuroprotective^[34-36] effects, among others^[37-39]. The therapeutic potential of COMs arises from their unique interactions with biological targets, making them valuable candidates for the treatment of various human diseases^[40]. The core structure of COM is associated with a distinctive pleasant aroma, while substitutions can take place at six specific positions^[41-43]. This structural feature, along with possible ring hybridization at different layouts, contribute to the extensive pharmacological diversity of COMs^[44-46]. In this context, COM-hybrid compounds have attracted significant global research attention for their potential bioactive properties^[47-49]. Extensive *in vitro* and *in vivo* studies are being conducted to evaluate these hybrids' therapeutic potential, with the aim of identifying effective candidates for the treatment of various diseases^[50]. Several studies have reported that COM-hybrid compounds exhibit bioactive properties, including antioxidant^[51-53], anticancer^[54-56], anti-inflammatory^[57-59], antidiabetic^[60-62], and antimicrobial effects^[63-66].

Heterocyclic compounds are cyclic organic molecules that include at least one heteroatom^[67] and the most common heteroatoms found in these compounds are nitrogen, oxygen, and sulfur^[68]. However, heterocyclic compounds containing other heteroatoms are also well known and widely studied^[69]. Heterocyclic compounds are essential in biology, particularly for their effectiveness in combating various diseases. Due to their significant role, heterocycles are extensively used in different biological applications and are recognized as a fundamental class of organic molecules^[70,71]. Also, heterocyclic compounds are integral to the structure of many vital biological molecules, such as chlorophyll, hemoglobin, vitamins, DNA, and RNA^[72]. Their structural diversity and unique properties make heterocycles highly valuable in medicinal chemistry, where they serve as key components in the development of numerous pharmaceutical drugs for treating various diseases^[73]. The heterocyclic structural features are present in over 90% of newly developed drugs, bridging the fields of biology and chemistry, where significant scientific discoveries and applications take place^[74]. The synthesis of various heterocyclic COM hybrids has attracted considerable attention from medicinal chemists due to their improved therapeutic applications^[75]. These hybrids are formed by strategically merging a COM ring with different heterocycles, including pyrrole^[76], furan^[77], pyran^[78], oxepine^[79], oxazole^[80], benzene with electron-donating^[81] or -withdrawing group^[82], dioxathiole^[83], and thiadiazole^[84]. This process, known as hybridization, involves incorporating the heterocyclic moiety as an integral part of the benzene and/or α -pyrone rings^[85]. Such an innovative approach to molecular modification has led to the development of hybrids with remarkable medicinal properties, offering promising prospects for therapeutic applications^[86].

The 1,3-dioxolane ring (DR) is a highly significant heterocyclic framework due to its broad applications in chemistry and pharmaceuticals^[87]. It serves as a versatile solvent^[88], a stabilizing agent in chemical reactions^[89], and a crucial precursor in drug synthesis^[90]. The distinct five-membered ring structure, characterized by the presence of two oxygen atoms, enhances the ring reactivity and adaptability^[91]. Furthermore, DR-based compounds demonstrate notable biological activities, making them valuable in the development of novel therapeutic agents^[92,93]. Many drugs that have a DR in their structure include antifungals (like ketoconazole and itraconazole), antivirals (like amdoxovir), and anticancer drugs (such as podophyllotoxin, etoposide, and teniposide)^[94,95]. These properties not only establish DR as a key component in both industrial and medicinal chemistry but also make it particularly effective in hybridization with COM, further expanding its potential applications^[96,97].

Although COMs have been extensively explored for their diverse biological activities, investigations specifically targeting the linear hybridization of DR with the coumarin scaffold remain scarce. To address this research gap, the present study focuses on the synthesis and pharmacological evaluation of a new series of DR-COM hybrid molecules (designated as **DCH1-DCH7**). These hybrids were designed to explore the therapeutic potential conferred by the integration of a DR into the COM framework. The synthetic route began with the preparation of a precursor molecule, **P-DCH**, which was subsequently modified to yield the lead

hybrid **DCH1**. Further structural diversification produced six additional analogs (**DCH2–DCH7**), as outlined in **Figure 1**. The resulting hybrids underwent a broad range of *in vitro* assays to determine their antioxidant, anticancer, anti-inflammatory, antidiabetic, and antimicrobial activities. In parallel, their biocompatibility was assessed using non-cancerous human cell lines and representative commensal bacterial strains. To complement the experimental findings, *in silico* evaluations of toxicity, drug-likeness, and pharmacokinetic parameters were also conducted, offering a comprehensive insight into their suitability as multi-target therapeutic candidates.

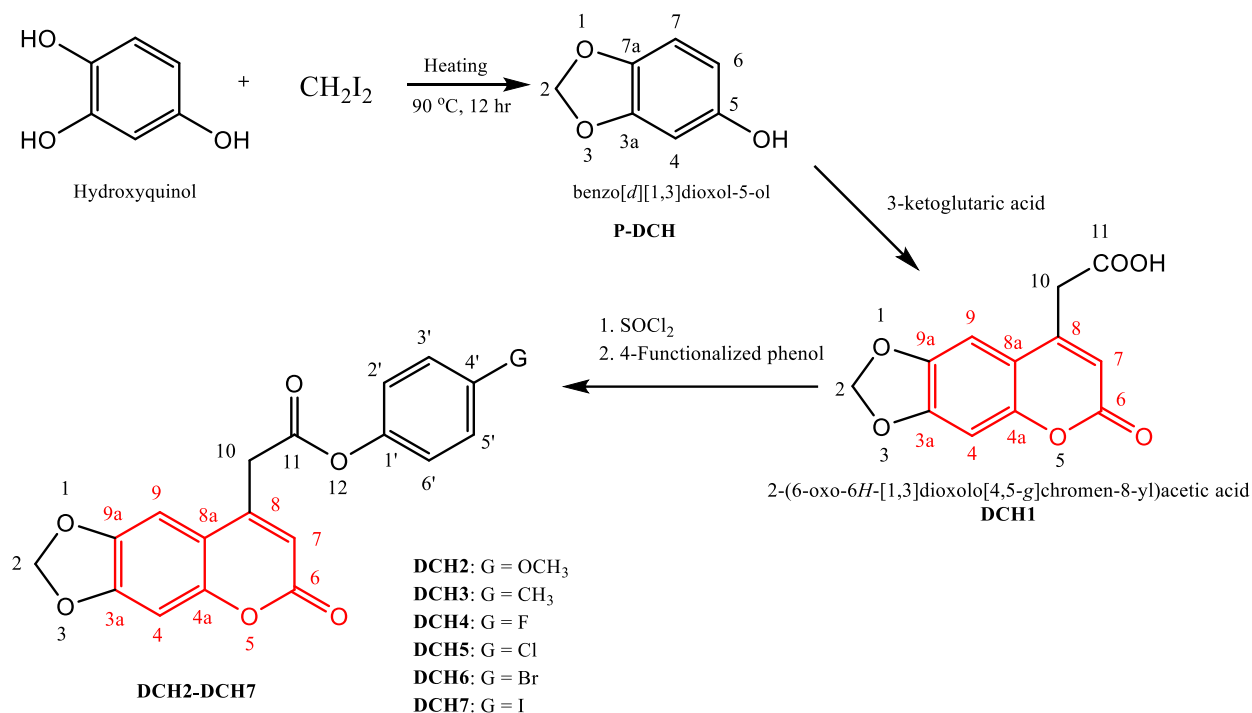


Figure 1. Synthetic pathway for the DR-COM hybrids.

2. Experimental section

2.1. Chemical materials, bioactive agents, and instruments

Several international suppliers were giving the scientists the chemicals and bioactive agents they needed to finish the process and investigate whether the synthesized DCHs could be used as medicines. BioVision, Bioworld, BT-LAB, Chambräu, Haihang, Key Organics Ltd, Labcorp, and Sigma-Aldrich were some of these suppliers. The quality of the synthesized ingredients was verified, and the development of the reactions was tracked using thin-layer chromatography (TLC). Given this technique, silica gel was used as the stationary phase, whereas acetone and chloroform were mixed in a 4:1 ratio to make the mobile phase. The instruments used were a α -brand Bruker ATR, an Avance III HD device (also made by Bruker) that runs at 75 MHz for ^{13}C and 300 MHz for ^1H , and a UV-1600PC Ultraviolet–Visible spectrophotometer. The purpose of these spectrophotometers was to measure the compounds' infrared, nuclear magnetic resonance, and ultraviolet–visible properties, respectively.

2.2. Synthesis of P-DCH

A solution of pyridine (0.40 ml, 5 mmol) and hydroxyquinol (1.26 g, 10 mmol) in 25 ml of anhydrous ethyl acetate was put in a salt-ice bath in a cone-shaped flask that was wrapped in aluminum foil to keep out light. A cold solution of diiodomethane (0.40 ml, 5 mmol) in 6 ml of anhydrous ethyl acetate was gradually added drop by drop as the mixture's temperature decreased to 0°C . After 12 hrs of mixing at 90°C , the reaction mixture was condensed, treated with 50 ml of H_2O , and the organic layer was isolated. Following dehydration

and reduced pressure vaporization, the named chemical was recovered by adding it to a crushed ice-water mixture, filtering it, and recrystallizing the solid with a combination of dichloromethane and ethanol^[98].

P-DCH: Off-white crystals; MP = 108-110°C; λ_{\max} (ethanol) = 292 nm; R_f = 0.17 (chloroform: acetone, in ratio of 4 to 1); percentage of yield (practical obtained weight) = 66.23 (0.46 g); IR ν_{\max} : 3206 cm^{-1} (broad band, hydrogen bonding phenolic O-H group), 2823 cm^{-1} (weak band, n-alkane C-H group), 1580 cm^{-1} (strong band, benzene C=C group), 1232 cm^{-1} and 1065 cm^{-1} (dioxolane ether C-O-C group); $^1\text{H-NMR}$ (DMSO- d_6 , 300 MHz): δ = 6.78 ppm (1H, doublet peak, J = 6 Hz, proton at position-7), 6.64 ppm (1H, doublet peak, J = 6 Hz, proton at position-6), 6.45 ppm (1H, singlet peak, proton at position-4), 5.96 ppm (2H, singlet peak, protons at position-2), and 5.52 ppm (1H, singlet peak, protons at position-5 of OH group); $^{13}\text{C-NMR}$ (DMSO- d_6 , 75 MHz): δ = 152.5 ppm (C, carbon at 5-position), 140.8 ppm (C, carbon at 7a-position), 138.4 ppm (C, carbon at 3a-position), 120.7 ppm (CH, carbon at 7-position), 113.9 ppm (CH, carbon at 6-position), 106.3 ppm (CH, carbon at 4-position), and 100.0 ppm (CH_2 , carbon at 2-position).

2.3. Synthesis of DCH1

A colorless ethyl acetate solution was obtained by gently heating 0.88 g of 3-ketoglutaric acid (6 mmol) with 0.69 g of **P-DCH** (5 mmol). The resulting mixture was slowly added to a round-bottom flask that held 25 ml of concentrated sulfuric acid while being kept below 10°C with a salty ice bath. The handling mixture was removed from this bath and allowed to sit on the stir plate at room temperature for the whole night after being continuously stirred for 2.5 hours. The next day, the mixture was transferred to a beaker and mixed with crushed ice and water. To obtain **DCH1**, the precipitate was gathered using filter paper, cold water-rinsed several times, and allowed to air-dry. The purification procedure used recrystallization from a combination of chloroform and ethanol (1:2)^[99].

DCH1: Off-white powder; MP = 153-155°C; λ_{\max} (ethanol) = 324 nm; R_f = 0.13 (chloroform: acetone, in ratio of 4 to 1); percentage of yield (practical obtained weight) = 86.17 (1.07 g); IR ν_{\max} : 3060 cm^{-1} (medium band, *cis* C=C group), 3013 cm^{-1} (broad band, hydrogen-bonding carboxylic acid O-H group), 2890 cm^{-1} (weak band, n-alkane C-H group), 1732 cm^{-1} (strong band, pyrone ring C=O group), 1690 cm^{-1} (strong band, C=O group of dimeric carboxylic acid), 1588 cm^{-1} (strong band, *cis* C=C group), 1546 cm^{-1} (medium band, benzene C=C group), 1228 cm^{-1} and 1065 cm^{-1} (dioxolane ether C-O-C group); $^1\text{H-NMR}$ (DMSO- d_6 , 300 MHz): δ = 11.11 ppm (1H, singlet peak, proton of O-H group), 6.91 ppm (1H, singlet peak, proton at position-4), 6.76 ppm (1H, singlet peak, proton at position-9), 6.35 ppm (1H, singlet peak, proton at position-7), 5.95 ppm (2H, singlet peak, proton at position-2), 3.10 ppm (2H, singlet peak, proton at position-10); $^{13}\text{C-NMR}$ (DMSO- d_6 , 75 MHz): δ = 173.1 ppm (C, carbon at 11-position), 162.2 ppm (C, carbon at 6-position), 153.0 ppm (C, carbon at 8-position), 146.4 ppm (C, carbon at 4a-position), 143.9 ppm (C, carbon at 3a-position), 141.5 ppm (C, carbon at 9a-position), 115.7 ppm (C, carbon at 7-position), 114.6 ppm (C, carbon at 8a-position), 113.5 ppm (CH, carbon at 9-position), 111.5 ppm (CH, carbon at 4-position), 100.0 ppm (CH_2 , carbon at 2-position), 30.9 ppm (CH_2 , carbon at 10-position).

2.4. General method for synthesizing DCH2-DCH7

In a salty ice bath, a round-bottom, dual-necked flask holding 1.24 g (5 mmol) of **DCH1** dissolved in 25 ml of fresh-distilled thionyl chloride was set up. A stopper supported with blue litmus paper was used to close off one of the necks, while a condenser was attached in the other. After stirring the mixture for 30 minutes in anhydrous circumstances, it was allowed to settle for another 30 minutes at room temperature before refluxing for 3 hours. The handling mixture was monitored for reaction endpoint using the blue-red color shift of the litmus paper that was changed every 30 minutes. Excess thionyl chloride was distilled once the blue litmus paper ceased changing color, and the production of the acyl chloride derivative of **DCH1** was evident from the leftover white substance in the flask. A 50 ml solution of dehydrated diethyl ether was added to the same flask that held the remaining white precipitate. This solution contains 5 mmol of 4-methoxyphenol, along with 1 ml

of pyridine. At room temperature, the addition was performed, and after 30 minutes of stirring in anhydrous circumstances, the mixture was refluxed. Furthermore, the litmus paper's color changes were employed to track the reaction's development. 50 ml of distilled water was added to the mixture once the reaction was finished. After that, the organic layer was separated, dried, and evaporated to produce **DCH2**. The other DCHs were synthesized in a manner like that of **DCH2**, but the only variance is the type of 4-functionalized phenol used. **So, methylphenol, fluorophenol, chlorophenol, bromophenol, and iodophenol were used to make DCH3, DCH4, DCH5, DCH6, and DCH7, in that order.** Chloroform and ethyl acetate mixed in a 2-to-1 ratio were used in the recrystallization process to purify each of the synthesized DCHs^[100].

DCH2: Pale yellowish-white powder; MP = 124-126°C; λ_{\max} (ethanol)= 372 nm; R_f = 0.53 (chloroform: acetone, in ratio of 4 to 1); percentage of yield (practical obtained weight) = 82.65 (1.46 g); IR ν_{\max} : 3095 cm^{-1} (medium band, *cis* C-H group), 2915 cm^{-1} (weak band, OMe C-H group), 2823 cm^{-1} (weak band, n-alkane C-H group), 1733 cm^{-1} (strong band, pyrone C=O group), 1710 cm^{-1} (strong band, non-aromatic ester C=O group), 1664 cm^{-1} (strong band, *cis* C=C group), 1593 cm^{-1} (strong band, benzene C=C group), 1266 cm^{-1} and 1064 cm^{-1} (dioxolane ether C-O-C group); $^1\text{H-NMR}$ (DMSO-*d*₆, 300 MHz): δ = 7.36 ppm (2H, doublet peak, J = 6 Hz proton at 3' and 5'- positions), 7.06 ppm (2H, doublet peak, proton at positions-2' and 6', J = 6 Hz), 6.91 ppm (1H, singlet peak, proton at position-4), 6.75 ppm (1H, singlet peak, proton at position-9), 6.36 ppm (1H, singlet peak, proton at position-7), 5.94 ppm (2H, singlet peak, proton at position-2), 4.14 ppm (3H, singlet peak, OMe group at position-4'), 3.14 ppm (2H, singlet peak, proton at position-10); $^{13}\text{C-NMR}$ (DMSO-*d*₆, 75 MHz): δ = 169.2 ppm (C, carbon at 11-position), 162.3 ppm (C, carbon at 6-position), 156.4 ppm (C, carbon at 4'-position), 153.0 ppm (C, carbon at 8-position), 146.4 ppm (C, carbon at 4a-position), 144.6 ppm (C, carbon at 1'-position), 143.9 ppm (C, carbon at 3a-position), 141.7 ppm (C, carbon at 9a-position), 124.0 ppm (CH, carbon at 4-position), 120.1 ppm (CH, carbon at 2' and 6'-positions), 115.7 ppm (CH, carbon at 3'-position, and carbon at 5'-position), 114.6 ppm (C, carbon at 8a-position), 113.4 ppm (CH, carbon at 7-position), 112.3 ppm (CH, carbon at 4-position), 100.1 ppm (CH₂, carbon at 2-position), 51.1 ppm (CH₃, OMe at 4'-position), 28.3 ppm (CH₂, carbon at 10-position).

DCH3: Pale yellowish-white powder; MP = 113-116°C; λ_{\max} (ethanol) = 363 nm; R_f = 0.50 (chloroform: acetone, in ratio of 4 to 1); percentage of yield (practical obtained weight) = 80.21 (1.36 g); IR ν_{\max} : 3087 cm^{-1} (medium band, *cis* C-H group), 2874 cm^{-1} (weak band, n-alkane C-H group), 2816 cm^{-1} (weak band, n-alkane C-H group), 1732 cm^{-1} (strong band, pyrone C=O group), 1711 cm^{-1} (strong band, non-aromatic ester C=O group), 1666 cm^{-1} (strong band, *cis* C=C group), 1594 cm^{-1} (strong band, benzene C=C group), 1219 cm^{-1} and 1068 cm^{-1} (dioxolane ether C-O-C group); $^1\text{H-NMR}$ (DMSO-*d*₆, 300 MHz): δ = 7.26 ppm (2H, doublet peak, J = 6 Hz, proton at position-3' and 5'), 7.03 ppm (2H, doublet peak, J = 6 Hz, proton at positions-2' and 6'), 6.90 ppm (1H, singlet peak, proton at position-4), 6.76 ppm (1H, singlet peak, proton at position-9), 6.37 ppm (1H, singlet peak, proton at position-7), 5.96 ppm (2H, singlet peak, proton at position-2), 3.13 ppm (2H, singlet peak, proton at position-10), 2.76 ppm (3H, singlet peak, OMe group at position-4'); $^{13}\text{C-NMR}$ (DMSO-*d*₆, 75 MHz): δ = 169.6 ppm (C, carbon at 11-position), 162.2 ppm (C, carbon at 6-position), 153.0 ppm (C, carbon at 8-position), 149.3 ppm (C, carbon at 1'-position), 146.5 ppm (C, carbon at 4a-position), 143.8 ppm (C, carbon at 3a-position), 141.7 ppm (C, carbon at 9a-position), 134.2 ppm (C, carbon at 4'-position), 122.0 ppm (CH, carbon at 3'-position and 5'-position), 119.0 ppm (CH, carbon at 2' and 6'-positions), 115.8 ppm (CH, carbon at 7-position), 114.6 ppm (C, carbon at 8a-position), 113.8 ppm (CH, carbon at 9-position), 111.5 ppm (CH, carbon at 4-position), 100.1 ppm (CH₂, carbon at 2-position), 27.5 ppm (CH₂, carbon at 10-position), and 24.1 ppm (CH₃, 4'-CH₃).

DCH4: White powder; MP = 138-141°C; λ_{\max} (ethanol) = 296 nm; R_f = 0.34 (chloroform: acetone, in ratio of 4 to 1); percentage of yield (practical obtained weight) = 51.09 (0.87 g); IR ν_{\max} : 3068 cm^{-1} (medium band, *cis* C-H group), 2823 cm^{-1} (weak band, n-alkane C-H group), 1733 cm^{-1} (strong band, pyrone C=O group), 1711 cm^{-1} (strong band, non-aromatic ester C=O group), 1664 cm^{-1} (strong band, *cis* C=C group), 1594 cm^{-1}

(strong band, benzene C=C group), 1217 cm^{-1} and 1064 cm^{-1} (strong band, dioxolane ether C-O-C group), 1095 cm^{-1} (strong band, benzene C-F group). $^1\text{H-NMR}$ (DMSO- d_6 , 300 MHz): $\delta = 7.26$ ppm (2H, doublet peak, $J = 6$ Hz, proton at position-2' and 6'), 7.04 ppm (2H, doublet peak, $J = 6$ Hz, proton at position-3', and 5'), 6.93 ppm (1H, singlet peak, proton at position-4), 6.77 ppm (1H, singlet peak, proton at position-9), 6.35 ppm (1H, singlet peak, proton at position-7), 5.94 ppm (2H, singlet peak, proton at position-2), 3.15 ppm (2H, singlet peak, proton at position-10); $^{13}\text{C-NMR}$ (75 MHz, DMSO- d_6): $\delta = 169.4$ ppm (C, carbon at 11-position), 162.7 ppm (C, carbon at 6-position), 158.2 ppm (C, carbon at 4'-position), 153.0 ppm (C, carbon at 8-position), 147.9 ppm (C, carbon at 4a-position), 146.5 ppm (C, carbon at 1'-position), 143.8 ppm (C, carbon at 3a-position), 141.7 ppm (CH, carbon at 9a-position), 120.7 ppm (CH, carbon at 2'-position and 6'-position), 115.8 ppm (CH, carbon at 3'-position and 5'-position), 114.7 ppm (C, carbon at 8a-position), 113.4 ppm (CH, carbon at 9-position), 111.5 ppm (CH, carbon at 7-position), 108.4 ppm (CH, carbon at 4-position), 100.0 ppm (CH_2 , carbon at 2-position), 27.5 ppm (CH_2 , carbon at 10-position).

DCH5: White powder; MP = 130-133°C; λ_{max} (ethanol) = 297 nm; $R_f = 0.35$ (chloroform: acetone, in ratio of 4 to 1); percentage of yield (practical obtained weight) = 55.12 (0.99 g) ; IR ν_{max} : 3065 cm^{-1} (medium band, *cis* C-H group), 2824 cm^{-1} (weak band, n-alkane C-H group), 1733 cm^{-1} (strong band, pyrone C=O group), 1710 cm^{-1} (strong band, non-aromatic ester C=O group), 1665 cm^{-1} (strong, *cis* C=C group), 1590 cm^{-1} (strong band, benzene C=C group), 1215 cm^{-1} and 1062 cm^{-1} (dioxolane ether C-O-C group), 983 cm^{-1} (benzene, C-Cl group); $^1\text{H-NMR}$ (DMSO- d_6 , 300 MHz): $\delta = 7.52$ ppm (2H, doublet peak, $J = 6$ Hz, proton at positions-3' and 5'), 7.32 ppm (2H, doublet peak, $J = 6$ Hz, proton at positions-2' and 6'), 6.91 ppm (1H, singlet peak, proton at position-4), 6.77 ppm (1H, singlet peak, $J = 6$ Hz, proton at position-9), 6.37 ppm (1H, singlet peak, proton at position-7), 5.95 ppm (2H, singlet peak, proton at position-2), 3.13 ppm (2H, singlet peak, proton at position-10); $^{13}\text{C-NMR}$ (DMSO- d_6 , 75 MHz): $\delta = 169.5$ ppm (C, carbon at 11-position), 162.2 ppm (C, carbon at 6-position), 153.0 ppm (C, carbon at 8-position), 150.4 ppm (C, carbon at 1'-position), 146.4 ppm (C, carbon at 4a-position), 143.9 ppm (C, carbon at 3a-position), 141.7 ppm (C, carbon at 9a-position), 132.0 ppm (C, carbon at 4'-position), 122.9 ppm (CH, carbon at 3' and 5'-positions), 120.5 ppm (CH, carbon at 2' and 6'-positions), 115.8 ppm (CH, carbon at 9-position), 114.1 ppm (CH, carbon at 8a-position), 113.4 ppm (CH, carbon at 7-position), 111.5 ppm (CH, carbon at 4-position), 100.1 ppm (CH_2 , carbon at 2-position), 33.2 ppm (CH_2 , carbon at 10-position).

DCH6: Slightly yellowish-white powder; MP = 117-119°C; λ_{max} (ethanol) = 310 nm; $R_f = 0.39$ (chloroform: acetone, in ratio of 4 to 1); percentage of yield (practical obtained weight) = 42.89% (0.86 g) ; IR ν_{max} : 3064 cm^{-1} (medium band, *cis* C-H group), 2824 cm^{-1} (weak band, n-alkane C-H group), 1731 cm^{-1} (strong band, pyrone C=O group), 1709 cm^{-1} (strong band, non-aromatic ester C=O group), 1666 cm^{-1} (strong band, *cis* C=C group), 1590 cm^{-1} (strong band, benzene C-C group), 1216 cm^{-1} and 1064 cm^{-1} (strong band, dioxolane ether C-O-C group), 896 cm^{-1} (strong band, benzene C-Br group); $^1\text{H-NMR}$ (DMSO- d_6 , 300 MHz): $\delta = 7.76$ ppm (2H, doublet peak, $J = 6$ Hz, proton at positions-3' and 5'), 7.16 ppm (2H, doublet peak, $J = 6$ Hz, proton at position-2' and 6'), 6.91 ppm (1H, singlet peak, proton at position-4), 6.75 ppm (1H, singlet peak, proton at position-9), 6.37 ppm (1H, singlet peak, proton at position-7), 5.95 ppm (2H, singlet peak, proton at position-2), 3.15 ppm (2H, singlet peak, proton at position-10); $^{13}\text{C-NMR}$ (DMSO- d_6 , 75 MHz): $\delta = 169.6$ ppm (C, carbon at 11-position), 162.2 ppm (C, carbon at 6-position), 153.0 ppm (C, carbon at 8-position), 151.3 (C, carbon at 1'-position), 146.6 ppm (C, carbon at 4a-position), 143.8 ppm (C, carbon at 3a-position), 141.7 ppm (C, carbon at 9a-position) 123.6 ppm (CH, carbon at 3'-position and carbon at 5'-position), 121.3 ppm (CH, carbon at 2'-position and carbon at 6'-position), 118.5 ppm (C, carbon at 4'-position), 115.8 ppm (CH, carbon at 9-position), 114.9 ppm (C, carbon at 8a-position), 113.4 ppm (CH, carbon at 7-position), 111.5 ppm (CH, carbon at 4-position), 100.1 ppm (CH_2 , carbon at 2-position), 33.3 ppm (CH_2 , carbon at 10-position).

DCH7: Slightly yellowish-white powder; MP = 110-112°C; λ_{max} (Ethanol) = 306; $R_f = 0.39$ nm (chloroform: acetone, in ratio of 4 to 1); percentage of yield (practical obtained weight) = 43.34% (0.98 g); IR

ν_{\max} : 3060 cm^{-1} (medium band, *cis* C-H group), 2827 cm^{-1} (weak band, n-alkane C-H group), 1731 cm^{-1} (strong band, pyrone C=O group), 1710 cm^{-1} (strong band, non-aromatic ester C=O group), 1663 cm^{-1} (strong band, *cis* C=C group), 1590 cm^{-1} (strong band, benzene C=C group), 1212 cm^{-1} and 1066 cm^{-1} (strong band, dioxolane ether C-O-C group), 796 cm^{-1} (strong band, benzene C-I); $^1\text{H-NMR}$ (DMSO- d_6 , 300 MHz): δ = 7.86 ppm (2H, doublet peak, J = 6 Hz, proton at position-3' and H-5'), 7.08 ppm (2H, doublet peak, J = 6 Hz, proton at position-2' and 6'), 6.91 ppm (1H, singlet peak, proton at position-4), 6.77 ppm (1H, singlet peak, proton at position-9), 6.36 ppm (1H, singlet peak, proton at position-7), 5.96 ppm (2H, singlet peak, proton at position-2), 3.13 ppm (2H, singlet peak, proton at position-10); $^{13}\text{C-NMR}$ (DMSO- d_6 , 75 MHz): δ = 169.4 ppm (C, carbon at 11-position), 162.2 ppm (C, carbon at 6-position), 153.0 ppm (C, carbon at 8-position), 151.2 ppm (C, carbon at 1'-position), 146.8 ppm (C, carbon at 4a-position), 143.8 ppm (C, carbon at 3a-position), 141.6 ppm (C, carbon at 9a-position), 129.6 ppm (CH, carbon at 3' and 5'-positions), 120.7 ppm (CH, carbon at 2' and 6'-position), 115.8 ppm (CH, carbon at 9-position), 114.6 ppm (C, carbon at 8a-position), 113.4 ppm (CH, carbon at 7-position), 111.5 ppm (CH, carbon at 4-position), 100.0 ppm (CH₂, carbon at 2-position), 93.0 ppm (C, carbon at 4'-position), 33.2 ppm (CH₂, carbon at 10-position).

3. Evaluation of biomedical activities

3.1. DCHs as anti-oxidative stress prospects

The SH-SY5Y human neuroblastoma cell line (ATCC: CRL-2266) was employed, with a starting cellular population of 12×10^3 . These cells were transferred from a growth plate containing DMEM/F-12 (brochure number 11320033) medium to a dark, flat-bottomed surface plate with 96 wells. After cultivation, the developed cells were exposed to an oxidative stressor, specifically 100 μM of H_2O_2 , for 24 hours. One of the chemicals under investigation was introduced to the cells at a concentration of 5 mM. The capacity of this chemical to mitigate the induced oxidative was quantified utilizing a reactive oxygen species-detecting kit (code Abcam ab 113,851). To simulate physiological conditions, an incubator maintained at a constant temperature of 37°C and a 5% CO_2 atmosphere was employed. Given the spectrophotometric evaluation, a redox-based fluorescent probe (SH0403 code) was employed to detect the formation of fluorescent green dichlorofluorescein, which results from the decomposition of diacetyl dichlorofluorescein by a biological enzyme. Furthermore, H_2O_2 (which is employed as a negative control) and DMF (employed as a positive control) were delivered separately to the generated SH-SY5Y cell lines. Subsequently, the treated cell lines were exposed to chloromethyl derivatives of diacetyl dichlorofluorescein (100 μM) for 1 hour, and the emitted fluorescence was computed via a fluorescent microscope^[101].

3.2. DCHs as anticancer prospects

The MTT method, which uses 3-[4, 5-dimethylthiazol-2-yl]-2,5-diphenyl tetrazolium bromide as a visible indicator, is used to test the anticancer activity of DCHs. All of the DCHs and the standard drug 5-fluorouracil (5-FU) were mixed with DMSO to make a blank solution with a concentration of 1 mg/ml. From this, the following nine distilled water-diluted concentrations were created: 3.12, 6.25, 12.5, 25, 50, 100, 200, 400, and 800 $\mu\text{g/ml}$. The chemicals being studied were also tested on six different types of cancer cells, which were named AMN3 (murine mammary cancer cells), HeLa (cervical epithelial cancer cells), KYSE-30 (human esophageal cancer cells), SKG (cervical squamous carcinoma cells), SK-OV-3 (ovarian cancer cells), and MCF-7 (breast cancer cells). In each well of a 96-well plate, 10,000 cells were cultured from every cancer cell line examined. Following a single day, the examined chemical was supplied to the treated wells in various concentrations. After 72 hours, the cells' viability was checked using a specific method: the medium was taken away, 28 μl of MTT solution (3.27 mM) was added, and the cells were then left to sit at 37°C for 90 minutes. The investigated (Ai) and control (Ac) wells were both assessed using the microplate reader, calibrated to a wavelength of 492 nm. This experiment was conducted 3 times for every chemical under investigation to ensure precision and optimize performance. To calculate the growth inhibition percentage (GI%), the formula

employed is $GI\% = [(Ac-Ai)/Ac] \times 100$. IC_{50} values were determined by nonlinear regression by putting the $GI\%$ data against their corresponding logarithmic concentration scores^[102].

3.3. DCHs as anti-inflammatory prospects

In this study, a COX enzyme model, comprising both COX-1 and COX-2 isoforms, was sourced from Cayman (catalog number: 560131) for evaluation. The test chemical, along with the reference drugs aspirin (Asp) and celecoxib (Cxb), was initially prepared as a DMSO solution at a concentration of 1 mg/ml. This stock solution was then serially diluted with distilled water to achieve final concentrations ranging from 3.12 to 800 $\mu\text{g/ml}$. There was 0.96 mL of 0.1 M Tris-HCl buffer in the reaction mixture, along with 10 μl of the enzyme preparation and 100 μl of the test chemical. Arachidonic acid, as a substrate, initiated the reaction after a 10-minute incubation at 37°C. Subsequently, 50 μl of Ellman's reagent (1 M) was introduced, allowing the reaction to proceed for an additional 2 minutes. Absorbance was then recorded at 410 nm using a spectrophotometer, with a blank control serving as the reference. The collected data were used to determine the IC_{50} values of the test compounds and their COX-1/COX-2 selectivity indexes^[103].

3.4. DCHs as antidiabetic prospects

The inhibitory potential of the synthesized DCHs against porcine α -amylase and yeast α -glucosidase was evaluated, with acarbose (ACB) serving as the reference standard. To achieve the desired test concentrations, the primary DMSO stock solution (2 mg/ml) was serially diluted with distilled water, generating seven sub-solutions ranging from 1000 to 25 $\mu\text{g/ml}$. The percentage inhibition (PS%), which reflects the antidiabetic activity, was calculated using the equation: $PS\% = (OPD_{ACB} - OPD_{SYN}) / OPD_{ACB} \times 100$. The OPD_{SYN} represents the optical density of the synthesized DCHs, and OPD_{ACB} corresponds to the optical density of ACB. The IC_{50} value of each compound was determined through nonlinear regression analysis by plotting PS% number against the corresponding logarithm of the concentration. Additionally, the potency coefficient (PC) of the synthesized DCHs was computed using the equation: $1 - (IC_{50} \text{ of the chemical under investigation} - IC_{50} \text{ of ACB}) / IC_{50} \text{ of ACB}$. This approach enabled the comparative assessment of the antidiabetic efficacy of the synthesized DCHs relative to ABC^[104].

3.5. Porcine α -amylase inhibitory assay

A phosphate-buffered solution (pH 6.8) was used to dissolve starch, preparing a substrate solution at a concentration of 500 $\mu\text{g/ml}$. At the same time, the enzyme solution was made by mixing 20 μl of the enzyme (2 units/ml) with the same amount of the test chemical at a known concentration. Subsequently, 40 μl of the substrate solution was mixed with the enzyme-test chemical mixture, and the reaction was incubated at 25°C for 10 minutes. To stop the enzyme reaction, 0.4 M sodium hydroxide, 12% anhydrous Rochelle salt, and 1% 2-hydroxy-3,5-dinitrobenzoic acid were added to the mixture while it was being stirred all the time. The mixture was then heated in a boiling water bath for 15 minutes, cooled to 25°C using tap water, and diluted to a final volume of 10 ml with distilled water. The test chemical's ability to stop the enzyme from working was found by measuring its absorbance at 540 nm. A blank control was prepared following the same procedure, except that distilled water was used in place of the test chemical solution^[105].

3.6. Yeast α -glucosidase inhibitory assay

4-nitrophenol- α -D-glucopyranoside was dissolved in a phosphate-buffered solution (pH 6.8) to make a 2 ml solution of the substrate mixture (375 $\mu\text{g/ml}$). At the same time, an enzyme mixture was made by mixing 20 μl of yeast α -glucosidase (0.1 unit/ml) with the same amount of a solution that had the right amount of the test chemical. Subsequently, 40 μl of the substrate mixture was mixed with 40 μl of the enzyme mixture, and the reaction was incubated at 37°C for 30 minutes. It was stopped by adding 80 μl of 0.2 M disodium carbonate in a buffered solution. The enzymatic activity was then assessed colorimetrically by measuring absorbance at

405 nm. A blank control was prepared using the same procedure, except that distilled water was used instead of the test chemical solution^[106].

4. DCHs as antimicrobial prospects

4.1. Anti-aerobic gram-negative bacterial potency

Six different types of aerobic gram-negative bacteria were tested to see how well the synthesized DCHs killed them using the broth dilution method. Mueller-Hinton broth served as the growth medium, while DMSO was used as the negative control, and ciprofloxacin (Cipro) was included as the positive control. To prepare the stock solution, 7.5 mg of the test compound was dissolved in 5 ml of DMSO. A series of 13 two-fold serial dilutions was then prepared using autoclaved distilled water as the diluent, yielding final concentrations ranging from 1024 µg/ml to 0.25 µg/ml. For each test, 3 ml of the broth, 0.2 ml of bacterial inoculum (adjusted to a 0.5 McFarland standard using autoclaved distilled water), and 1 ml of the respective dilution were combined in labeled test tubes. The tubes were then incubated at 37°C for 24 hours, after which bacterial growth was assessed visually. The lowest concentration at which no visible bacterial growth was observed was recorded as the minimum inhibitory concentration (MIC). To determine the minimum bactericidal concentration (MBC), an aliquot from just above-MIC dilution (based on 4, 1, 0.5, or 0.05 dilution factor) was sub-cultured onto fresh broth-containing test tubes and incubated under the same conditions. The MBC was defined as the lowest concentration at which no bacterial growth was detected. The potency marker (PM) of each compound was calculated by dividing its MBC value by the corresponding MIC value^[107].

4.2. Anti-anaerobic bacterial potency

The methodology used to evaluate the potency of DCHs against four kinds of pathogenic anaerobic bacteria largely mirrored the approach applied to assess their effectiveness against gram-negative bacterial strains, albeit with some key modifications. Notably, metronidazole (Metro) served as the positive control, and Brucella agar supplemented with 5% sheep blood was utilized as the growth medium. Furthermore, the incubation period was extended to 48 hours at 37°C within an anaerobic jar. This jar maintained an atmosphere composed of 10% H₂, 10% CO₂, and 80% N₂, ensuring anaerobic conditions. To facilitate this environment, a palladium catalyst and an anaerobe indicator were incorporated^[108].

4.3. Antifungal potency

The steps used to test how well the DCHs killed two kinds of pathogenic fungi were very similar to the steps used to test how well they killed aerobic gram-negative bacteria. The main differences were that the minimum fungicidal concentration (MFC) was used as the main measure of antifungal activity, Sabouraud dextrose broth was used as the growth medium, and nystatin (Nyst) served as the reference antifungal agent. The incubation period was extended to 48 hours by maintaining the temperature at 30°C to ensure optimal fungal growth conditions^[109].

5. DCHs as biocompatible prospects

5.1. Biosafety toward commensal bacterial strains

The biosafety evaluation of DCHs was conducted using three commensal bacterial strains, employing the same broth dilution method previously used for assessing aerobic gram-negative bacteria. Mueller-Hinton Broth was utilized as the growth medium, while Cipro served as the positive control and DMSO as the negative control. Additionally, the MIC, MBC, and PM were determined following the same investigational working steps^[110].

5.2. Biosafety toward non-cancerous cell lines

After evaluating the anticancer potential of DCHs, a biosafety assessment was conducted. The first phase of the study utilized an MTT-based colorimetric assay to examine the cytotoxic effects of these chemicals against six different tumor cell lines, aiming to determine their potential anticancer activity. In the subsequent phase, the carcinogenicity of the chemicals under assessment was detected using a similar methodological approach. However, instead of cancer cells, three non-cancerous cell lines, including human prostatic epithelial cells (RWPE-1), human mammary epithelial cells (MCF-10A), and human embryonic renal cells (HEK-293), were employed to evaluate their effects on normal cellular viability and safety^[111].

6. Algorithmic assessment of pharmacological suitability

6.1. Preliminary assessment of simulated toxicology

The ProTox-II platform was utilized to evaluate the computerized theoretical toxicity of DCHs. This assessment was conducted by analyzing their chemical structures and comparing them to known compounds within the platform's extensive database. ProTox-II uses predictive algorithms to guess toxicity classes and find possible interactions with enzymes that are involved in toxicity. This open-source tool provides useful information about the safety profile of newly synthesized chemicals, which helps with preliminary toxicity screening before more experiments are done to confirm the results^[112].

6.2. Preliminary assessment of simulated pharmacokinetics and drug-likeness

The PreADME and SwissADME online-predicting tools were utilized to computerize the theoretical assessment of the pharmacokinetics and drug-likeness in relation to DCHs. Researchers can use these platforms for free to look at molecular properties based on the two-dimensional structure of chemicals; this makes them useful for early drug screening. These prediction tools give a lot of computer-generated data, like how well chemicals dissolve in water, how well they dissolve in fat, how bioavailable they are, how well they move through membranes, and other pharmacokinetic and drug-related properties that are important for preliminary research^[113].

7. Results and discussion

7.1. Synthetic approach

The synthetic pathway employed in this study (**Figure 1**) involved a series of well-defined steps. Initially, diiodomethane was reacted with hydroquinone to generate the intermediate **P-DCH**. This compound subsequently underwent a Pechmann condensation with 3-ketoglutaric acid to afford **DCH1**, which was then converted into a series of ester derivatives, **DCH2–DCH7**, via esterification of its acyl chloride intermediate with various substituted phenols. The acyl chloride was prepared by treating **DCH1** with thionyl chloride. It is worth noting that halogen-substituted phenols, due to the electron-withdrawing nature of halogens, exhibit reduced nucleophilicity. As a result, such esterification reactions are less frequently reported in the literature. Nevertheless, careful optimization of reaction conditions in the present study led to successful synthesis of the targeted compounds with satisfactory yields^[114].

Compared to the methodology reported by Nameer et al.^[115], the current synthetic route demonstrates several improvements. These include the selection of more effective solvents, refined reaction conditions, and a more efficient purification process. Notably, our approach eliminates the need for an additional dehydration step involving calcium chloride, which was necessary in the Nameer et al. protocol. Instead, the reaction was carried out in anhydrous ethyl acetate, which offered superior solubility and stability, thereby promoting consistent reaction kinetics. A key advantage of the present method lies in the use of diiodomethane for the initial transformation, as opposed to thionyl chloride used by Nameer et al. Furthermore, our procedure

incorporates an extended reaction period—12 hours at 90 °C—as opposed to only 3 hours of stirring at 0 °C, as described in the previous method. This prolonged reaction time contributed to improved yields and more complete conversions.

Throughout the synthesis, the progression of acyl chloride formation was monitored using litmus paper, allowing for precise control of reaction progress. Additionally, purification was enhanced by crystallizing the final products from a dichloromethane–ethanol mixture (1:2 ratio), which significantly improved both yield and purity when compared to the ethyl acetate-based purification used in the earlier method. Overall, the optimized conditions presented in this study—particularly with regard to solvent selection, reaction duration, and purification—resulted in a more robust and reliable synthetic approach, delivering higher product quality and greater efficiency than previously reported methods.

7.2. DCHs and their anti-oxidative stress capacity

Recent scientific advancements have firmly established the link between oxidative stress and various age-related diseases, including cancer, cardiovascular conditions, chronic inflammation, and other health issues^[116–118]. In light of this, the present study evaluated the potential of synthesized hybrids to alleviate oxidative stress in human SH-SY5Y cell populations exposed to H₂O₂. To ensure a comprehensive assessment, DMF, H₂O₂, and a combination of DMF and H₂O₂ were used as the positive control, negative control, and reference, respectively. Intracellular reactive oxygen species (iROS) levels, induced by H₂O₂ exposure and subsequently modulated by the synthesized hybrids, were quantified and are presented in **Table 1**.

The study highlighted three key observations, the most prominent of which was the notable antioxidant activity exhibited by compounds bearing phenyl ester moieties—especially **DCH4**—whose efficacy was comparable to that of the standard reference compound. This suggests that such hybrid molecules may hold therapeutic promise for managing diseases linked to oxidative stress. Secondly, while the DCHs demonstrated antioxidant effects, their potency was generally lower than that of the reference agent, with effective concentrations ranging between 228 and 328 µg/ml. Thirdly, the compounds' antioxidant efficacy followed the order: **DCH4** > **DCH5** > **DCH2** > **DCH3** > **DCH6** > **DCH7** > **DCH1**. The superior activity of **DCH4** is likely attributed to the presence of a fluorine substituent on the phenyl ester group, enhancing its oxidative stress mitigation potential. In contrast, **DCH1** showed the weakest activity, possibly due to the absence of a phenyl ester moiety. **DCH2** and **DCH5** also exhibited promising activity, which may be linked to the presence of methoxy and chloro substituents, respectively. **DCH3** and **DCH6** demonstrated moderate activity, associated with methyl and bromo groups, while the relatively low activity of **DCH7** might stem from the influence of the iodo substituent. Overall, these findings underscore the importance of structural modifications in influencing antioxidant performance and support the potential of these hybrid molecules as scaffolds for future drug development targeting oxidative stress-related conditions.

Table 1. The results in relative fluorescence units ± standard deviation (n = 3) from studying how DCHs might work as antioxidants.

Compound	iROS
Positive control (DMF)	181.27 ± 1.08
Negative control (H ₂ O ₂)	523.76 ± 1.23
Reference (H ₂ O ₂ +DMF)	211.83 ± 1.00
DCH1	328.45 ± 1.14
DCH2	234.85 ± 1.20
DCH3	253.68 ± 0.98
DCH4	228.52 ± 0.86
DCH5	230.02 ± 1.16
DCH6	310.33 ± 1.24
DCH7	311.76 ± 1.11

7.3. DCHs and their anticancer capacity

The anticancer potential of the synthesized hybrid compounds was evaluated using the MTT assay across six distinct human cancer cell lines: AMN-3, HeLa, KYSE-30, SKG, SK-OV-3, and MCF-7. **Table 2** presents the half-maximal inhibitory concentration (IC_{50}) values for each hybrid compound alongside 5-FU, a well-established chemotherapeutic agent used as the reference standard^[119]. The IC_{50} values served as the basis for interpreting the cytotoxic efficacy of the compounds. Initial IC_{50} values for the synthesized hybrids ranged from 13.28 $\mu\text{g/ml}$ to 102.29 $\mu\text{g/ml}$, indicating varying degrees of cytotoxic activity. All compounds demonstrated a similar mode of action. Among them, **DCH4** emerged as the most potent, followed by **DCH5**, **DCH2**, **DCH3**, **DCH6**, **DCH7**, and finally **DCH1**, which exhibited the weakest anticancer activity across all tested cell lines. Notably, the limited efficacy of the latter compound highlights the importance of the phenyl ester moiety in enhancing anticancer activity.

Hybrids containing electron-withdrawing halogen substituents, particularly fluoride (**DCH4**) and chloride (**DCH5**), demonstrated pronounced cytotoxic effects. The former one was especially effective, displaying strong inhibitory activity against multiple cell lines—most notably HeLa, MCF-7, and SK-OV-3—suggesting its potential as a promising lead compound for further oncological research. **DCH5** also exhibited substantial anticancer activity, reinforcing its potential value. Conversely, hybrids substituted with methoxy and methyl groups (**DCH2** and **DCH3**) showed moderate efficacy, while those containing bromide and iodide (**DCH6** and **DCH7**) were among the least active. Interestingly, the fluoride-substituted compound **DCH4** demonstrated cytotoxic effects comparable to those of 5-FU in cell lines such as MCF-7 and HeLa, and showed similar potency against AMN-3 and SK-OV-3. The superior activity of this hybrid compound may be attributed to the strong electron-withdrawing nature of the fluoride group, which is known to influence molecular interactions with biological targets. This observation aligns with previous reports linking aromatic fluoride substitution to enhanced anticancer properties^[120–122].

Table 2. The results as IC_{50} ($\mu\text{g/ml}$) \pm standard deviation ($n = 3$) from studying how DCHs might work as anticancer prospects.

Cell line	Compound							
	5-FU	DCH1	DCH2	DCH3	DCH4	DCH5	DCH6	DCH7
AMN-3	25.2 \pm 1.04	63.52 \pm 1.14	53.95 \pm 0.94	68.54 \pm 1.02	29.89 \pm 0.98	32.24 \pm 1.04	62.85 \pm 1.06	69.39 \pm 1.00
HeLa	13.45 \pm 1.18	60.64 \pm 1.12	19.16 \pm 1.04	37.50 \pm 0.94	13.65 \pm 1.02	16.87 \pm 1.07	51.57 \pm 1.02	52.40 \pm 1.17
KYSE-30	31.26 \pm 1.11	69.07 \pm 0.93	49.55 \pm 1.06	53.41 \pm 1.026	44.21 \pm 0.95	44.36 \pm 1.10	56.56 \pm 1.09	59.55 \pm 1.03
MCF-7	12.56 \pm 1.12	92.65 \pm 1.07	23.68 \pm 1.17	29.89 \pm 1.02	13.28 \pm 1.17	23.80 \pm 1.17	85.47 \pm 0.97	90.70 \pm 1.10
SKG	22.53 \pm 1.18	102.29 \pm 0.9486	43.18 \pm 1.14	38.60 \pm 1.19	33.15 \pm 1.09	33.25 \pm 1.02	83.93 \pm 1.01	80.29 \pm 1.10
SK-OV-3	22.96 \pm 0.97	64.29 \pm 0.95	58.09 \pm 1.01	38.42 \pm 0.91	26.21 \pm 0.88	30.30 \pm 0.89	56.51 \pm 1.03	62.77 \pm 0.97

7.4. DCHs and their anti-inflammatory capacity

The synthesized hybrid compounds were evaluated for their anti-inflammatory potential by assessing their inhibitory effects on the cyclooxygenase enzymes COX-1 and COX-2^[123,124]. Asp and Cxb were employed as reference standards^[125], and the half-maximal inhibitory IC_{50} values for both the standard drugs and the synthesized compounds are summarized in **Table 3**. Several important observations emerged from the data. Firstly, the hybrid molecules demonstrated comparatively lower COX inhibitory activity than the reference drugs. However, their mode of action appeared to be similar. The IC_{50} values for the synthesized compounds ranged from 102.10 $\mu\text{g/ml}$ to 224.82 $\mu\text{g/ml}$. Notably, the order of inhibitory potency among the hybrids was as follows: **DCH1** > **DCH4** > **DCH5** > **DCH2** > **DCH3** > **DCH6** > **DCH7**.

Among the tested compounds, **DCH1** exhibited the most potent inhibition against both COX-1 and COX-2. Its superior activity is likely attributed to the absence of a phenyl ester moiety, which may enhance its interaction with the enzyme active sites. **DCH4** and **DCH5** also displayed notable activity, though to a lesser extent, possibly due to the presence of fluorine and chlorine substituents on the phenyl ester ring. Compounds **DCH2** and **DCH3** showed moderate inhibition, which could be linked to their methoxy and methyl substitutions, respectively. In contrast, **DCH6** and **DCH7** exhibited the weakest inhibitory effects, potentially due to the presence of bulkier halogen substituents such as bromine and iodine. Furthermore, the COX-1/COX-2 selectivity among the hybrids followed the trend: **DCH7** > **DCH6** > **DCH1** = **DCH2** = **DCH3** > **DCH5** > **DCH4**. The COX-1/COX-2 selectivity ratios suggest that several of the synthesized compounds, particularly **DCH1**, may serve as promising scaffolds for further structural refinement in the pursuit of novel anti-inflammatory agents. These findings also highlight the significance of the heterocyclic core structure in modulating enzyme selectivity and inhibitory activity.

Table 3. The results as IC₅₀ (µg/ml) ± standard deviation (n = 3) from studying how DCHs might work as anti-inflammatory prospects.

Test name	Compound								
	Asp	Cxb	DCH1	DCH2	DCH3	DCH4	DCH5	DCH6	DCH7
COX-1	3.80 ± 0.88	7.45 ± 0.96	123.30 ± 0.87	196.38 ± 0.89	196.09 ± 0.86	186.54 ± 0.91	187.29 ± 0.93	223.85 ± 0.84	224.82 ± 0.96
COX-2	31.24 ± 0.96	1.78 ± 0.90	102.10 ± 0.87	161.75 ± 0.93	161.83 ± 0.84	130.56 ± 1.06	142.39 ± 1.04	188.43 ± 1.17	192.18 ± 0.97
COX-1/CoX-2 selectivity marker	0.12	4.19	1.21	1.21	1.21	1.43	1.32	1.19	1.17

7.5. DCHs and their antidiabetic capacity

An *in vitro* investigation was conducted to evaluate the antidiabetic potential of the synthesized hybrid compounds by assessing their inhibitory activity against two key enzymes involved in carbohydrate metabolism: porcine α -amylase and yeast α -glucosidase^[126]. ACB was employed as the standard reference drug for comparison., while the IC₅₀ values, which reflect the degree of enzyme inhibition, are summarized in **Table 4** for both the test compounds and the reference. The analysis revealed several noteworthy observations. Overall, the synthesized hybrids exhibited moderate inhibitory activity relative to ACB. Specifically, their IC₅₀ values against yeast α -glucosidase ranged from 376.11 µg/ml to 438.31 µg/ml, while inhibition of porcine α -amylase was observed in the range of 339.99 µg/ml to 388.31 µg/ml. Despite being less potent than ACB, the hybrids demonstrated consistent inhibitory effects on both enzymes, suggesting a uniform mechanism of action.

The compounds followed a distinct order of potency based on their IC₅₀ values: **DCH2** > **DCH3** > **DCH1** > **DCH4** > **DCH5** > **DCH6** > **DCH7**. Among these, **DCH2** and **DCH3** emerged as the most promising candidates, likely due to the presence of electron-donating substituents such as methoxy and methyl groups at the C-4" position. These groups, when integrated into a conjugated framework, may enhance electron density and facilitate stronger interactions with the enzyme active sites, thereby improving inhibitory activity. Conversely, **DCH6** and **DCH7** exhibited the lowest antidiabetic activity. This diminished potency may be attributed to the incorporation of electron-withdrawing atoms like bromine and iodine at the same C-4" position, which could reduce the compounds' ability to interact effectively with the target enzymes. These findings underscore the importance of structural modifications, particularly the nature and position of substituents on the phenyl ring, in modulating antidiabetic efficacy. While the heterocyclic core contributes to the biological activity, strategic functionalization can significantly influence therapeutic potential. Based on these insights, **DCH2** and **DCH3** represent valuable scaffolds for the design of more potent α -amylase and α -glucosidase inhibitors for potential use in diabetes management.

Table 4. The results as IC₅₀ (µg/ml) ± standard deviation (n = 3) from studying how DCHs might work as antidiabetic prospects.

Test name	Compound							
	ACB	DCH1	DCH2	DCH3	DCH4	DCH5	DCH6	DCH7
Procine α-amylase Potency factor-1	263.63 ± 0.94	362.83 ± 0.97	339.99 ± 1.05	348.61 ± 0.96	368.07 ± 0.98	368.55 ± 0.98	386.10 ± 1.03	388.31 ± 1.06
Yeast α-glucosidase Potency factor-2	283.22 ± 0.89	409.82 ± 1.02	376.11 ± 0.92	379.31 ± 1.05	416.96 ± 0.99	427.71 ± 0.96	436.15 ± 0.95	438.31 ± 1.00
	1.00	0.73	0.78	0.76	0.72	0.72	0.68	0.68
	1.00	0.69	0.75	0.75	0.68	0.66	0.65	0.65

8. DCHs and their antimicrobial properties

8.1. Anti-aerobic gram-negative bacterial capacity

This study evaluated the synthesized hybrids for their antibacterial activity *in vitro* against six gram-negative bacterial strains using the microdilution technique in a broth medium. The tested strains included *Klebsiella pneumoniae* (ATCC 700603), *Pseudomonas aeruginosa* (ATCC 27853), *Escherichia coli* (ATCC 25922), *Haemophilus influenzae* (ATCC 49247), *Shigella dysenteriae* (ATCC 13313), and *Salmonella typhi* (ATCC 6539)^[127]. **Table 5** presents the MIC, MBC, and PM values for each hybrid as well as the reference drug. While the hybrid compounds demonstrated noteworthy antibacterial activity against the tested gram-negative bacterial strains, their potency was generally lower than that of Cipro. The MIC values for the hybrids ranged from 2.50 µg/ml to 18.00 µg/ml, and the MBC values spanned from 3.50 µg/ml to 35.00 µg/ml.

The descending order of antibacterial activity was observed as follows: **DCH5** > **DCH2** > **DCH3** > **DCH4** > **DCH6** > **DCH7** > **DCH1**. This trend suggests that increasing the hydrophobic character of the hybrids enhanced their effectiveness against gram-negative pathogens^[128,129]. Notably, **DCH5** emerged as the most potent among the series, exhibiting bactericidal activity across all tested strains. Its superior performance is likely attributed to its structural features—specifically, the presence of a 4-chlorophenyl group at the C-4" position. This group may enhance membrane permeability and interaction with bacterial targets due to its dual hydrophilic and lipophilic nature, along with its ability to act as a hydrogen bond acceptor^[130,131].

DCH2 also exhibited strong antibacterial activity, albeit slightly lower than that of **DCH5**. Compounds **DCH3** and **DCH4** showed moderate efficacy, possibly due to the influence of methoxy, methyl, and fluorine substituents. In contrast, **DCH6** and **DCH7** displayed reduced activity, which may be attributed to the presence of bulkier halogens like bromine and iodine. The least effective hybrid, **DCH1**, contained a carboxylic acid group at the C-1' position—a strongly hydrophilic moiety that may hinder its ability to penetrate bacterial membranes^[132]. Despite the variability in potency, all synthesized hybrids exhibited bactericidal properties against the tested gram-negative strains, as reflected in their PM values, which ranged from 1.20 to 2.44.

Table 5. The results from studying how DCHs might work as anti-aerobic gram-negative bacterial prospects.

Bacterial strain	Test name	Cipro	DCH1	DCH2	DCH3	DCH4	DCH5	DCH6	DCH7
<i>Escherichia coli</i>	MIC	0.85	18.00	5.00	9.00	9.00	2.50	8.00	12.00
	MBC	1.65	35.00	7.00	11.00	11.00	3.50	12.00	24.00
	PM	1.94	1.94	1.40	1.22	1.22	1.40	1.50	2.00
<i>Haemophilus influenzae</i>	MIC	1.05	18.00	5.00	8.00	9.00	2.50	8.00	9.00
	MBC	1.85	24.00	6.00	11.00	11.00	3.50	17.00	22.00
	PM	1.76	1.33	1.20	1.38	1.22	1.40	2.13	2.44
<i>Klebsiella pneumoniae</i>	MIC	0.65	9.00	5.00	5.00	5.00	2.50	9.00	11.00
	MBC	1.35	17.00	7.00	11.00	9.00	3.00	13.00	17.00

Bacterial strain	Test name	Cipro	DCH1	DCH2	DCH3	DCH4	DCH5	DCH6	DCH7
<i>Salmonella typhi</i>	PM	2.08	1.89	1.40	2.20	1.80	1.20	1.44	1.55
	MIC	1.85	18.00	4.00	9.00	9.00	2.50	9.00	18.00
	MBC	2.75	23.00	8.00	12.00	12.00	3.50	13.00	23.00
<i>Shigella dysenteriae</i>	PM	1.49	1.28	2.00	1.33	1.33	1.40	1.44	1.28
	MIC	0.65	18.00	4.00	8.00	5.00	2.50	9.00	17.00
	MBC	1.20	27.00	8.00	11.00	7.00	4.00	16.00	25.00
<i>Pseudomonas aeruginosa</i>	PM	1.85	1.50	2.00	1.38	1.40	1.60	1.78	1.47
	MIC	1.15	18.00	4.00	4.00	4.00	2.50	9.00	10.00
	MBC	1.95	22.00	6.00	10.00	7.00	3.00	14.00	22.00
PM	1.70	1.22	1.50	2.50	1.75	1.20	1.56	2.20	

Table 5. (Continued)

The values of MIC and MBC are expressed in the unit of $\mu\text{g/ml}$

8.2. Anti-anaerobic bacterial capacity

This study examined the antibacterial activity of the synthesized hybrids against four anaerobic bacterial strains: *Clostridium perfringens* (ATCC 13124), *Bacteroides fragilis* (ATCC 25285), *Prevotella melaninogenica* (ATCC 25845), and *Fusobacterium necrophorum* (ATCC 25286)^[133]. The anti-anaerobic bacterial parameters for each tested compound as well as the reference drug are detailed in **Table 6**. The results revealed that the synthesized hybrid compounds exhibited comparatively lower antibacterial activity than Metro. Despite this, they appeared to operate through a similar fashion of action. The MIC values ranged from 7.00 $\mu\text{g/ml}$ to 57.00 $\mu\text{g/ml}$, while the MBC values varied between 9.00 $\mu\text{g/ml}$ and 91.00 $\mu\text{g/ml}$. Based on their MIC matrixes, the compounds were ranked as follows: **DCH2** > **DCH3** > **DCH5** > **DCH4** > **DCH1** > **DCH7** > **DCH6**.

Interestingly, these hybrids showed improved anti-anaerobic activity when compared with earlier reports on linear benzocoumarins^[134], highlighting the significance of incorporating heterocyclic structures in enhancing antibacterial efficacy. Among the tested series, **DCH2** emerged as the most potent, likely due to the presence of a methoxy group at the C-4" position, which may contribute to its superior activity against anaerobic bacteria. On the other hand, **DCH6** was the least effective, potentially due to the presence of a bromine substituent at the same position. This substitution appears to diminish its antibacterial potency, as indicated by the relatively high MIC and MBC values required to inhibit and eliminate bacterial growth. These findings underscore the potential for further structural optimization, particularly of **DCH2**, to enhance its therapeutic effectiveness against anaerobic pathogens.

Table 6. The results from studying how DCHs might work as anti-anaerobic bacterial prospects.

Bacterial strain	Test name	Metro	DCH1	DCH2	DCH3	DCH4	DCH5	DCH6	DCH7
<i>Bacteroides fragilis</i>	MIC	3.00	52.00	10.00	17.00	33.00	32.00	57.00	53.00
	MBC	3.50	78.00	11.00	22.00	41.00	41.00	68.00	64.00
	PM	1.17	1.50	1.10	1.29	1.24	1.28	1.19	1.21
<i>Clostridium perfringens</i>	MIC	1.05	53.00	7.00	11.00	30.00	28.00	44.00	33.00
	MBC	1.85	68.00	9.00	14.00	35.00	33.00	59.00	41.00
	PM	1.76	1.28	1.29	1.27	1.17	1.18	1.34	1.24
<i>Fusobacterium necrophorum</i>	MIC	2.00	35.00	8.00	13.00	35.00	26.00	40.00	48.00
	MBC	2.65	91.00	9.00	15.00	50.00	33.00	46.00	55.00

Bacterial strain	Test name	Metro	DCH1	DCH2	DCH3	DCH4	DCH5	DCH6	DCH7
<i>Prevotella melaninogenica</i>	PM	1.33	2.60	1.13	1.15	1.43	1.27	1.15	1.15
	MIC	0.95	48.00	10.00	13.00	40.00	35.00	48.00	53.00
	MBC	1.55	91.00	12.00	17.00	59.00	46.00	55.00	68.00
	PM	1.63	1.90	1.20	1.31	1.48	1.31	1.15	1.28

Table 6. (Continued)

The values of MIC and MBC are expressed in the unit of $\mu\text{g/ml}$

8.3. Antifungal capacity

A Sabouraud dextrose broth dilution assay was conducted to evaluate the antifungal activity of the synthesized hybrids in comparison to Nyst against two pathogenic fungal strains: *Aspergillus niger* (ATCC 16888) and *Candida albicans* (ATCC 10231)^[135]. **Table 7** summarizes the antifungal parameters for the tested hybrids as well as the reference antifungal drug. The synthesized hybrid compounds exhibited a broad spectrum of antifungal activity, with MIC values ranging from 1.45 $\mu\text{g/ml}$ to 33.00 $\mu\text{g/ml}$ and MFC values spanning 1.75 $\mu\text{g/ml}$ to 39.00 $\mu\text{g/ml}$. Among these, the presence of a heterocyclic core appeared to significantly influence antifungal potency. For instance, **DCH1** demonstrated superior antifungal activity compared to the standard drug Nyst. Furthermore, the antifungal effectiveness of hybrids bearing 4-substituted phenyl rings varied depending on the nature of the substituent groups. Compounds **DCH4** and **DCH5**, which incorporate fluoro- and chloro-substituted phenyl moieties, showed notable antifungal efficacy, indicating their promise as scaffolds for the development of new antifungal agents. In contrast, **DCH6** and **DCH7**, containing bromo- and iodo-substituted phenyl groups, were the least active, as evidenced by their relatively high MIC and MFC values^[136].

Table 7. The results from studying how DCHs might work as antifungal prospects.

Fungal strain	Test name	Nyst	DCH1	DCH2	DCH3	DCH4	DCH5	DCH6	DCH7
<i>Aspergillus niger</i>	MIC	8.00	1.45	11.00	13.00	1.90	2.00	31.00	33.00
	MFC	11.00	1.75	15.00	17.00	2.25	3.00	35.00	39.00
	PM	1.38	1.21	1.36	1.31	1.18	1.50	1.13	1.18
<i>Candida albicans</i>	MIC	4.00	1.25	6.00	4.00	1.50	1.75	18.00	19.00
	MFC	6.00	1.50	7.00	7.00	1.75	2.00	19.00	21.00
	PM	1.50	1.20	1.17	1.75	1.17	1.14	1.06	1.11

The values of MIC and MFC are expressed in the unit of $\mu\text{g/ml}$

9. DCHs and their biocompatibility aspects

9.1. Biosafety toward commensal bacterial strains

Most orally administered prescription drugs have a negative impact on the normal growth of gut microbiota, often leading to side effects such as diarrhea^[137]. To test this idea with the new hybrids, researchers looked at how they affected the growth of normal microbiota using three types of friendly *Escherichia coli*: BAA-1427, BAA-1430, and MG1655. In this study, Cipro was used as a reference agent for two key reasons: first, because it is an approved oral antibiotic, and second, to validate the reliability of the testing method^[138]. **Table 8** presents the antimicrobial activity of the synthesized hybrid compounds alongside Cipro. Based on toxicity assessments, the hybrids were ranked from least to most toxic as follows: **DCH5**, **DCH1**, **DCH4**, **DCH3**, **DCH6**, **DCH7**, and **DCH2**. Notably, Cipro exhibited a strong inhibitory effect on the growth of the tested commensal bacterial strains. In contrast, the hybrid compounds—particularly **DCH5**—demonstrated

considerably lower bactericidal activity against these beneficial microbes. Nonetheless, all the tested hybrids showed potent bactericidal effects, as evidenced by their low PM values, which may pose potential biosafety concerns. These findings highlight the need for further comprehensive studies to better understand and evaluate their safety profiles^[139].

Table 8. The results from investigating the microbiota biocompatibility aspect of the DCHs.

Bacterial strain	Test name	Cipro	DCH1	DCH2	DCH3	DCH4	DCH5	DCH6	DCH7
<i>Escherichia coli</i> (BAA-1427)	MIC	1.05	13.00	7.00	11.00	12.00	16.00	9.00	9.00
	MBC	1.35	16.00	11.00	14.00	14.00	22.00	12.00	11.00
	PM	1.29	1.23	1.57	1.27	1.17	1.38	1.33	1.22
<i>Escherichia coli</i> (BAA1430)	MIC	1.15	11.00	12.00	17.00	18.00	23.00	11.00	11.00
	MBC	1.55	14.00	15.00	21.00	22.00	28.00	16.00	13.00
	PM	1.35	1.27	1.25	1.24	1.222	1.22	1.45	1.18
<i>Escherichia coli</i> (MG1655)	MIC	1.60	15.00	12.00	18.00	21.00	27.00	11.00	12.00
	MBC	2.00	18.00	14.00	22.00	24.00	30.00	12.00	15.00
	PM	1.25	1.20	1.17	1.22	1.14	1.11	1.09	1.25

The values of MIC and MBC are expressed in the unit of $\mu\text{g/ml}$

9.2. Biosafety toward non-cancerous cell lines

To assess the cellular biosafety of the synthesized hybrids, the same MTT assay was conducted on three noncancerous cell lines: RWPE-1, MCF-A10, and HEK-293. As a positive control, 5-FU—a well-established anticancer agent—was used. Several important findings can be drawn from the data presented in **Table 9**. Firstly, the IC_{50} values of 5-FU against noncancerous cell lines closely aligned with those reported in previous studies, thereby validating the reliability of the employed experimental protocol^[140]. The biosafety range observed for the tested compounds extended from 48.10 $\mu\text{g/ml}$ to 149.73 $\mu\text{g/ml}$. Notably, all synthesized hybrid compounds demonstrated markedly improved biosafety profiles in comparison to the standard drug, 5-FU. Among them, **DCH4** emerged as the most potent anticancer agent, displaying a biosafety index nearly threefold higher than that of 5-FU. This suggests a promising degree of selectivity for cancer cells and underscores the potential of this hybrid for further mechanistic and preclinical evaluation.

Table 9. The results as IC_{50} ($\mu\text{g/ml}$) \pm standard deviation ($n = 3$) from investigating the cellular biocompatibility aspect of the DCHs.

Cell line	Compound							
	5-FU	DCH1	DCH2	DCH3	DCH4	DCH5	DCH6	DCH7
HEK-293	41.43 \pm	51.22 \pm	69.09 \pm	61.43 \pm	136.41 \pm	67.86 \pm	55.34 \pm	48.10 \pm
	1.13	0.97	1.03	0.94	1.06	1.10	0.96	1.18
MCF-A10	42.47 \pm	53.89 \pm	71.61 \pm	63.30 \pm	149.73 \pm	73.07 \pm	58.84 \pm	54.80 \pm
	0.89	1.04	1.10	1.18	1.13	0.94	0.96	1.03
RAPE-1	34.75 \pm	48.29 \pm	66.01 \pm	57.80 \pm	134.94 \pm	96.20 \pm	52.94 \pm	48.76 \pm
	1.08	1.06	1.12	0.94	1.20	1.14	0.97	0.94

9.3. Computer-aided drug eligibility characteristics

9.3.1. Anticipated toxicity parameters

A principal obstacle hindering the advancement and accessibility of many research studies in the applied medical field was the potential toxicity of specific synthetic compounds^[141]. Numerous computer-aided systems have been created to predict the probable toxicity of various synthetic compounds^[142,143]. The present research employed the ProTox-II system to predict the toxicity profiles of the synthesized hybrids. The toxicity-related terminology derived from this system is described in **Table 10**. Before interpreting the statistics, it is evident that the average similarity percentage ranged from 51.22% to 59.02%. This signifies the

originality of the synthesized hybrid, as there were no closely related compounds in the platform's dataset. Nevertheless, this minimal percentage may result in diminished expected accuracy (below 70%), as this platform relies on structural resemblance between dataset architectures and the analyzed hybrid structures to predict the toxicity profile for the compounds. The estimated LD50 values for the synthesized hybrids are ranged between 3200 mg/kg and 1500 mg/kg. Since these values fall within the 500–5000 mg/kg range, the hybrids are considered slightly toxic based on LD50 classification. Their predicted toxicity levels correspond to categories 4 and 5, which help assess the overall chemical toxicity profile. In this scale, a higher level (closer to 6) indicates lower toxicity. Based on these findings, the synthetic hybrids demonstrate an acceptable toxicity profile^[144,145].

In medicinal chemistry, the topological polar surface area (TPSA) is an important measure of a molecule's polarity. It is calculated based on the surface area occupied by polar atoms or functional groups within the molecule. TPSA is closely linked to a compound's ability to pass through biological membranes and enter cells. Generally, non-polar molecules have low TPSA values (below 20 Å²), while highly polar molecules, which contain multiple functional groups such as hydroxyl, amine, carbonyl, and carboxyl, can have TPSA values reaching several hundred Å²^[146]. For the synthesized hybrids, TPSA values ranged from 74.97 Å² to 85.97 Å², suggesting a well-balanced lipophilicity that promotes efficient absorption in the intestines. At the same time, their pronounced polarity likely restricts their ability to penetrate the blood–brain barrier, which may help reduce potential toxicity to the central nervous system, and the other hybrids that have penetration may help in central nervous system agent scaffolds^[147].

Also, the data listed in **Table 10** indicates that all hybrids did not exhibit liver toxicity; this illustrates the evident role of halogens in the liver toxicity of the produced hybrids. The synthesized hybrids exhibit no significant potential for carcinogenicity, immunogenicity (all synthesized hybrids have no effect on immunogenicity except **DCH2** and **DCH4**), or cytotoxicity. Eventually, the created hybrids **DCH1**, **DCH5**, **DCH6**, and **DCH7** don't cause any alteration, while **DCH2**, **DCH3**, and **DCH4** possess the capacity to induce alterations in DNA sequences, leading to mutations. The chance of such mutations occurring was reported to be minimal. Consequently, further research is required to validate the toxicity of these hybrids^[148].

Table 10. The computer-based toxicity prediction regarding the synthesized hybrids.

Applicable principle toxicity	Compound						
	DCH1	DCH2	DCH3	DCH4	DCH5	DCH6	DCH7
A-Tox-level	5	4	4	4	4	4	4
Car-Tox	0.61	0.65	0.66	0.62	0.61	0.62	0.61
Cyt-Tox	0.8	0.82	0.82	0.69	0.69	0.71	0.71
Imm-Tox	0.96	0.56	0.88	0.61	0.53	0.57	0.76
Liver-Tox	0.78	0.77	0.77	0.56	0.55	0.56	0.57
Mut-Tox	0.56	0.58	0.54	0.53	0.52	0.54	0.53

A-Tox-level: Anticipated toxicity level, Liver-Tox: Liver toxicity, Car-Tox: Carcinogenicity, Imm-Tox: Immunogenicity, Mut-Tox: Mutagenicity, and Cyt-Tox: Cytotoxicity.

9.3.2. Anticipated pharmacokinetic parameters

Many computational analyses have been created to provide insights into the pharmacokinetic characteristics of the compounds being studied since drug development and discovery are intricate and varied processes^[149,150]. This work employed the pre-ADMET and SwissADMET platforms to report the pharmacokinetic parameters of the synthesized hybrids. **Table 11** shows the information that was gathered after the chemical structures of the synthesized hybrids were sent to these two different online search engines. Although the synthesized hybrids achieve nearly complete intestinal absorption, the permeability of Caco2

cells constrains their deficient internal diffusion values. This discovery indicates that the intestinal absorption process may utilize other techniques beyond energy-independent mechanisms. One reason could be that the absorption rates in Caco-2 cell models are different from those in other intestinal cells because they lack certain transporters, extracellular mediators (like phospholipids and bile acids), or mucus-secreting cellular components^[151].

The ability to inhibit the P-glycoprotein pump was confirmed by each of the synthesized hybrids^[152]. This inhibition can boost bioavailability by augmenting gastrointestinal medication absorption. Nonetheless, this activity-inhibiting effect retains the capacity to create drug removal or effects associated with interaction^[153]. When it comes to their ability to stop metabolizing enzymes, all of the synthesized hybrids were able to stop CYP3A4 and CYP2C9 but not **DCH1**. Concerning CYP2D6, all DCHs exhibited no inhibitory effects. It is important to be careful when giving these new hybrids along with other drugs that depend on the metabolism of the CYP3A4 subfamily^[154]. This subfamily is important for the metabolism of about half of the medicines on the market right now^[155]. This warning aims to mitigate the potential dangers linked to medication interactions.

Overall, the synthesized hybrids had better protein binding capacities and ranks (52.828–96.839%), which meant that the volume of distribution was smaller, the half-life was longer, and the percentage of unbound proteins was lower^[156]. The strong ability to bind to plasma proteins can change how the medicine works and how it behaves, since only the part of the drug that is not bound can have an effect on living things^[157]. The fact that the synthesized hybrids have a low ability to pass through the blood-brain barrier suggests that they will not be very toxic and probably won't have any negative effects on the nervous system, which is in line with their TPSA values. The seldom manifestation of adverse effects is essential in evaluating the level of toxicity to the central nervous system^[158]. All synthesized hybrids conform to Lipinski's Rule of Five, signifying their suitability as potential candidates for oral administration^[159].

Table 11. The online pharmacokinetic prediction regarding the synthesized hybrids.

Pharmacokinetic parameters	DCH1	DCH2	DCH3	DCH4	DCH5	DCH6	DCH7
BBB	No	No	Yes	Yes	Yes	Yes	Yes
BA	0.56	0.55	0.55	0.55	0.55	0.55	0.55
CaCP	21.076	33.357	31.195	30.377	25.604	24.779	24.759
CYP3A4	No	Yes	Yes	Yes	Yes	Yes	Yes
CYP2C9	No	Yes	Yes	Yes	Yes	Yes	Yes
CYP2D6	No						
GDA%	High 89.343	High 98.852	High 98.843	High 98.822	High 98.539	High 98.045	High 97.917
LR-5	Applicable						
P-gp	No						
PPB	52.828	86.917	90.025	88.352	90.509	90.495	96.839
PWS	1.86e-00 mg/ml	3.49e-02 mg/ml	2.05e-02 mg/ml	3.86e-02 mg/ml	1.14e-02 mg/ml	1.11e-02 mg/ml	1.36e-02 mg/ml
SF	2.82	3.36	3.32	3.19	3.19	3.21	3.35

BBB: Capacity to cross the blood–brain barrier, CaCP: Caco2 cell permeability in nm/sec, CYP: Cytochrome-P450, BA: Bioavailability, GDA%: Percentage of gastric drug absorption, LR-5: Lipinski's rule of five, P-gp: Capability to bypass the glycoprotein pumping, PPB: Extent of plasma protein binding, PWS: predicted water solubility in mg/ml, and SF: synthetic feasibility.

10. Conclusion

The investigation into 1,3-dioxolane-coumarin hybrid compounds (**DCH1–DCH7**) has yielded promising results that underscore their potential as multi-target therapeutic agents. The improved way of making these compounds, with better control over the reactions and purification, led to the creation of very pure compounds, which helped in conducting accurate biological tests. Each assay provided critical insights: the antioxidant studies revealed that hybrids with electron-withdrawing groups—particularly **DCH4**—offer enhanced protection against oxidative stress, a key factor in many degenerative conditions. In anticancer assessments, **DCH4** and **DCH5** emerged as the most potent, suggesting that the nature and position of substituents on the phenyl ester moiety are crucial for cytotoxic efficacy. The anti-inflammatory tests, although showing moderate enzyme inhibition compared to standard drugs, highlighted the role of the heterocyclic core in modulating COX-1 and COX-2 enzyme activity; **DCH1** is a strong anti-inflammatory and antifungal. Furthermore, the antidiabetic evaluations indicated that **DCH2** and **DCH3** possess a balanced inhibition of porcine α -amylase and yeast α -glucosidase, making them potential leads for glycemic control. The antimicrobial assays confirmed a broad-spectrum activity against both aerobic and anaerobic bacteria, **DCH5** and **DCH2** being stronger, respectively, with efficacy varying according to structural modifications. Importantly, biosafety assessments showed that these compounds exert minimal adverse effects on non-cancerous cells and commensal microorganisms, finding **DCH4** and **DCH5** to be stronger agents, respectively. Complementary *in silico* studies further validated the pharmacokinetic suitability and low toxicity of the hybrids. Overall, these results create a strong basis for improving and developing 1,3-dioxolane-coumarin hybrids in drug discovery.

Conflict of interest

The authors declare no conflict of interest.

About the author

Duha Adnan Hassan, duha.23php30@student.uomosul.edu.iq, <http://orcid.org/0009-0003-4895-1120>;

Yasser Fakri Mustafa, Dr.yassermustafa@uomosul.edu.iq, <http://orcid.org/0000-0002-0926-7428>

References

1. Elmusa F, Elmusa M. Mini-Review on Coumarins: Sources, Biosynthesis, Bioactivity, Extraction and Toxicology. *Journal of the Turkish Chemical Society Section A: Chemistry*. 2024;11(3):933–44.
2. Jasim SF, Mustafa YF. A Review of Classical and Advanced Methodologies for Benzocoumarin Synthesis. *Journal of Medicinal and Chemical Sciences*. 2022;5(5):676–94.
3. Annunziata F, Pinna C, Dallavalle S, Tamborini L, Pinto A. An overview of coumarin as a versatile and readily accessible scaffold with broad-ranging biological activities. *International Journal of Molecular Sciences*. 2020;21(13):1–83.
4. Tsvileva OM, Koftin O V, Evseeva N V. Coumarins as Fungal Metabolites with Potential Medicinal Properties. *Antibiotics*. 2022;11(9):1156.
5. Khalil RR, Mohammed ET, Mustafa YF. Various promising biological effects of Cranberry extract: A review. *Clinical Schizophrenia and Related Psychoses*. 2021;15(S6):1–9.
6. Sharifi-Rad J, Cruz-Martins N, López-Jornet P, Lopez EPF, Harun N, Yeskalyeva B, Beyatli A, Sytar O, Shaheen S, Sharopov F, Taheri Y, Docea AO, Calina D, Cho WC. Natural Coumarins: Exploring the Pharmacological Complexity and Underlying Molecular Mechanisms. Gil G, editor. *Oxidative Medicine and Cellular Longevity*. 2021;2021:6492346.
7. Ismael RN, Mustafa YF, Al-Qazaz HK. *Citrullus lanatus*, a Potential Source of Medicinal Products: A Review. *Journal of Medicinal and Chemical Sciences*. 2022;5(4):607–18.
8. Kasim SM, Al-Dabbagh BM, Mustafa YF. A review on the biological potentials of carbazole and its derived products. *Eurasian Chemical Communications*. 2022;4(6):495–512.
9. Mustafa YF. Biocompatible chlorocoumarins from harmful chlorophenols, their synthesis and biomedical evaluation. *Journal of Molecular Structure*. 2024;1309:138193.
10. Ahmed BA, Mustafa YF, Ibrahim BY. Isolation and characterization of furanocoumarins from Golden Delicious apple seeds. *Journal of Medicinal and Chemical Sciences*. 2022;5(4):537–45.

11. Younes AH, Mustafa YF. Plant-Derived Coumarins: A Narrative Review Of Their Structural And Biomedical Diversity. *Chemistry & Biodiversity*. 2024;21(6):e202400344.
12. Mustafa YF. Nutraceutical-based telomerase inhibitors: Renewed hope for cancer therapy. *Phytomedicine Plus*. 2024;4(2):100537.
13. Younes HA, Mustafa YF. Sweet Bell Pepper: A Focus on Its Nutritional Qualities and Illness-Alleviated Properties. *Indian Journal of Clinical Biochemistry*. 2024;39:459–69.
14. Mustafa YF, Khalil RR, Mohammed ET. Synthesis and antitumor potential of new 7-halocoumarin-4-acetic acid derivatives. *Egyptian Journal of Chemistry*. 2021;64(7):3711–6.
15. Mustafa YF. Synthesis, characterization and preliminary cytotoxic study of sinapic acid and its analogues. *Journal of Global Pharma Technology*. 2019;11(9):1–10.
16. Mustafa YF, Najem MA, Tawffiq ZS. Coumarins from Creston apple seeds: Isolation, chemical modification, and cytotoxicity study. *Journal of Applied Pharmaceutical Science*. 2018;8(8):49–56.
17. Younes AH, Mustafa YF. Novel coumarins from green sweet bell pepper seeds: Their isolation, characterization, oxidative stress-mitigating, anticancer, anti-inflammatory, and antidiabetic properties. *Journal of Molecular Structure*. 2024;1312:138629.
18. Mustafa YF, Mohammed ET, Khalil RR. Synthesis, characterization, and anticoagulant activity of new functionalized biscoumarins. *Egyptian Journal of Chemistry*. 2021;64(8):4461–8.
19. Zeki NM, Mustafa YF. Natural linear coumarin-heterocyclic conjugates: A review of their roles in phytotherapy. *Fitoterapia*. 2024;175:105929.
20. Flores-Morales V, Villasana-Ruíz AP, Garza-Veloz I, González-Delgado S, Martínez-Fierro ML. Therapeutic Effects of Coumarins with Different Substitution Patterns. *Molecules*. 2023;28(5):2413.
21. Al-Shakarchi W, Abdulaziz NT, Mustafa YF. A review of the chemical, pharmacokinetic, and pharmacological aspects of quercetin. *Eurasian Chemical Communications*. 2022;4(7):645–56.
22. Keri RS, Budagumpi S, Balappa Somappa S. Synthetic and natural coumarins as potent anticonvulsant agents: A review with structure–activity relationship. *Journal of Clinical Pharmacy and Therapeutics*. 2022;47(7):915–31.
23. Mahmood AAJ, Mustafa YF, Abdulstaar M. New coumarinic azo-derivatives of metoclopramide and diphenhydramine: Synthesis and in vitro testing for cholinesterase inhibitory effect and protection ability against chlorpyrifos. *International Medical Journal Malaysia*. 2014;13(1):3–12.
24. Abdulaziz NT, Al-bazzaz FY, Mustafa YF. Natural products for attenuating Alzheimer’s disease: A narrative review. *Eurasian Chemical Communications*. 2023;5(4):358–70.
25. Mustafa YF. Synthesis, in silico analysis, and biomedical effects of coumarins derived from resveratrol. *Phytomedicine Plus*. 2024;3(4):100501.
26. Mustafa YF. Role of Fruit-Derived Antioxidants in Fighting Cancer: A Narrative Review. *Indian Journal of Clinical Biochemistry*. 2025;e70321. <https://doi.org/10.1007/s12291-025-01310-7>
27. Alshaher MM, Mustafa YF. Linear pyranocoumarins are potential dazzling dancers between nature, chemistry, and clinical application. *Phytomedicine Plus*. 2025;5(2):100785.
28. Mohammed ET, Khalil RR, Mustafa YF. Phytochemical Analysis and Antimicrobial Evaluation of Quince Seeds’ Extracts. *Journal of Medicinal and Chemical Sciences*. 2022;5(6):968–79.
29. Hachem K, Jasim SA, Al-Gazally ME, Riadi Y, Yasin G, Turki Jalil A, Abdulkadh MM, Saleh MM, Fenjan MN, Mustafa YF, Dehno Khalaji A. Adsorption of Pb(II) and Cd(II) by magnetic chitosan-salicylaldehyde Schiff base: Synthesis, characterization, thermal study and antibacterial activity. *Journal of the Chinese Chemical Society*. 2022;69(3):512–21.
30. Roomi AB, Widjaja G, Savitri D, Jalil AT, Mustafa YF, Thangavelu L, Kazhibayeva G, Suksatan W, Chupradit S, Aravindhan S. SnO₂:Au/Carbon Quantum Dots Nanocomposites: Synthesis, Characterization, and Antibacterial Activity. *Journal of Nanostructures*. 2021;11(3):514–23.
31. Mustafa YF. Effects of heat variables on the starch content of cooked white rice: Searching for diabetes-friendly food. *Bioactive Carbohydrates and Dietary Fibre*. 2024;31:100395.
32. Al Abdeen SHZ, Mustafa YF, Mutlag SH. Synthesis and biomedical activities of novel multifunctional benzodipyronone-based derivatives. *Eurasian Chemical Communications*. 2022;4(10):938–49.
33. Abdulaziz NT, Mohammed ET, Khalil RR, Mustafa YF. Unrevealing the total phenols, total flavonoids, antioxidant, anti-inflammatory, and cytotoxic effects of Garden Cress seed ethanolic extracts. *Review of Clinical Pharmacology and Pharmacokinetics - International Edition*. 2024;38(2):187–96.
34. Mustafa YF, Al-Shakarchi W. The psychotropic potential of coumarins: Mechanisms, efficacy, and future prospects. *Environment and Social Psychology*. 2025;10(3):3534.
35. Jebir RM, Mustafa YF. Watermelon Allsweet: A promising natural source of bioactive products. *Journal of Medicinal and Chemical Sciences*. 2022;5(5):652–66.
36. Huldani H, Rashid AI, Turaev KN, Oplencia MJC, Abdelbasset WK, Bokov DO, Mustafa YF, Al-Gazally ME, Hammid AT, Kadhim MM, Ahmadi SH. Concanavalin A as a promising lectin-based anti-cancer agent: the molecular mechanisms and therapeutic potential. *Cell Communication and Signaling*. 2022;20(1):1–14.
37. Mustafa YF, Khalil RR, Mohammed ET, Bashir MK, Oglah MK. Effects of structural manipulation on the bioactivity of some coumarin-based products. *Archives of Razi Institute*. 2021;76(5):1297–305.

38. Mustafa YF, Oglah MK, Bashir MK, Mohammed ET, Khalil RR. Mutual prodrug of 5-ethynyluracil and 5-fluorouracil: Synthesis and pharmacokinetic profile. *Clinical Schizophrenia and Related Psychoses*. 2021;15(5):1–6.
39. Rohmah MK, Salahdin OD, Gupta R, Muzammil K, Qasim MT, Al-qaim ZH, Abbas NF, Jawad MA, Yasin G, Mustafa YF, Heidary A, Abarghouei S. Modulatory role of dietary curcumin and resveratrol on growth performance, serum immunity responses, mucus enzymes activity, antioxidant capacity and serum and mucus biochemicals in the common carp, *Cyprinus carpio* exposed to abamectin. *Fish and Shellfish Immunology*. 2022;129:221–30.
40. Riaz M, Khalid R, Afzal M, Anjum F, Fatima H, Zia S, Rasool G, Egbuna C, Mtewa AG, Uche CZ, Aslam MA. Phytobioactive compounds as therapeutic agents for human diseases: A review. *Food Science & Nutrition*. 2023;11(6):2500–29.
41. Elmusa S, Elmusa M, Elmusa B, Kasımoğulları R. Coumarins: Chemical Synthesis, Properties and Applications. *Düzce Üniversitesi Bilim ve Teknoloji Dergisi*. 2025;13(1):131–70.
42. Abdulaziz NT, Mustafa YF. The Effect of Heat Variable on the Chemical Composition and Bioactivities of a *Citrullus lanatus* Seed Aqueous Extracts. *Journal of Medicinal and Chemical Sciences*. 2022;5(7):1166–76.
43. Zeki NM, Mustafa YF. Coumarin hybrids: a sighting of their roles in drug targeting. *Chemical Papers*. 2024;78:5753–5772.
44. Gangopadhyay A. Plant-derived natural coumarins with anticancer potentials: future and challenges. *Journal of Herbal Medicine*. 2023;42:100797.
45. Zeki NM, Mustafa YF. Synthesis and Pharmacological Profiles of 6,7-Dihydroxycoumarin and Its Derivatives: A Concise Review. *Iraqi Journal of Pharmacy*. 2023;20(Supplementary Issue 1):174–88.
46. Jibroo RN, Mustafa YF. Linearly ring-fused coumarins: A review of their cancer-fighting attributes. *Results in Chemistry*. 2024;8:101611.
47. Kumari S, Sharma A, Yadav S. Coumarin Chalcone Hybrids: Molecular Hybridization Strategy for Drug Design. *International Research Journal of Multidisciplinary Scope*. 2024;5(3):321–30.
48. Jibroo RN, Mustafa YF, Al-Shakarchi W. Heterocycles fused on a 6,7-coumarin framework: an in-depth review of their structural and pharmacological diversity. *Chemical Papers*. 2024;78:7239–7311.
49. Al Abdeen SHZ, Mustafa YF, Mutlag SH. Synthesis of disubstituted anisodipyronederived ester compounds: The search for new bioactive candidates. *Eurasian Chemical Communications*. 2022;4(11):1171–83.
50. Mustafa YF, Hassan DA, Faisal AF, Alshaher MM. Synthesis of novel skipped diene-3-halocoumarin conjugates as potent anticancer and antibacterial biocompatible agents. *Results in Chemistry*. 2024;11:101846.
51. Yildirim M, Poyraz S, Ersatir M. Recent advances on biologically active coumarin-based hybrid compounds. *Medicinal Chemistry Research*. 2023;32:617–42.
52. Faisal AF, Mustafa YF. Capsicum in Clinical Biochemistry: Insights into its Role in Health and Disease. *Indian Journal of Clinical Biochemistry*. 2025; <https://doi.org/10.1007/s12291-025-01317-0>
53. Mazin Zeki N, M. Z. Othman K, Mustafa YF. Computational Chemistry: A game-changer in the drug discovery field. *Applied Chemical Engineering*. 2025;8(1):5601.
54. Shaik BB, Katari NK, Seboletswe P, Gundla R, Kushwaha ND, Kumar V, Singh P, Karpoornath R, Bala MD. Recent Literature Review on Coumarin Hybrids as Potential Anticancer Agents. *Anti-Cancer Agents in Medicinal Chemistry*. 2023;23(2):142–63.
55. Rawat A, Vijaya Bhaskar Reddy A. Recent advances on anticancer activity of coumarin derivatives. *European Journal of Medicinal Chemistry Reports*. 2022;5:100038.
56. Faisal AF, Mustafa YF. The role of coumarin scaffold in the chemical engineering of bioactive molecules: A narrative review. *Applied Chemical Engineering*. 2025;8(1):5595.
57. Mustafa YF. Coumarins derived from natural methoxystilbene as oxidative stress-related disease alleviators: Synthesis and in vitro-in silico study. *Journal of Molecular Structure*. 2024;1302:137471.
58. Nibin Joy M, Guda MR, Zyryanov G V. Evaluation of Anti-Inflammatory and Anti-Tubercular Activity of 4-Methyl-7-Substituted Coumarin Hybrids and Their Structure Activity Relationships. *Pharmaceuticals*. 2023;16(9):1326.
59. Mustafa YF, Hassan DA. Dioxolocoumarins: Bridging chemistry and pharmacology with multifunctional therapeutics. *Applied Chemical Engineering*. 2024;7(4):5592.
60. Nandu Rangnath Kayande, Nitin Ashok Lodhe, Samadhan Kundlik Magar, Arun Balabhau Mante, Amol Ramesh Lahane, Amol Ramesh Lahane, Nilesh Prakashrao Sawadadkar. A review on medicinal plants for the management of diabetes mellitus. *World Journal of Biology Pharmacy and Health Sciences*. 2024;19(2):062–5.
61. Faisal AF, Mustafa YF. The Multifaceted Chemistry of Chili Peppers: A Biodiversity Treasure for Nutrition and Biomedicine. *Chemistry & Biodiversity*. 2025; <https://doi.org/10.1002/cbdv.202402690>
62. Faisal AF, Mustafa YF. Chili pepper: A delve into its nutritional values and roles in food-based therapy. *Food Chemistry Advances*. 2025;6:100928.
63. Mustafa YF. Emerging trends and future opportunities for coumarin-heterocycle conjugates as antibacterial agents. *Results in Chemistry*. 2023;6:101151.
64. Li WB, Qiao XP, Wang ZX, Wang S, Chen SW. Synthesis and antioxidant activity of conjugates of hydroxytyrosol and coumarin. *Bioorganic Chemistry*. 2020;105:104427.

65. Ban AA, Ibrahim BY, Mustafa YF. The Protective Role of Natural Coumarins Derivatives and Anpro Supplement Against Aflatoxin B1 Pollution in the Quails Coturnix Japonica Diet. *Mesopotamia Journal of Agriculture*. 2023;51(1):1–13.
66. Alshaher MM, Mustafa YF. Synthesis of triclosan-derived coumarins as potent, biocompatible, broad-spectrum antimicrobial agents. *Applied Chemical Engineering*. 2024;7(4):5579.
67. Borissov A, Maurya YK, Moshniaha L, Wong WS, Żyła-Karwowska M, Stępień M. Recent Advances in Heterocyclic Nanographenes and Other Polycyclic Heteroaromatic Compounds. *Chemical Reviews*. 2022;122(1):565–788.
68. Rana R, Ansari A. Synthesis of 7-Membered Heterocyclic Compounds and Their Biological Activity. *Journal of Physics: Conference Series*. 2023;2603(1):012058.
69. Jain KP, Utekar M, Shinde Y. A Review on Heterocyclic Compounds. 2023;7(10):21–6.
70. Amewu RK, Sakyi PO, Osei-Safo D, Addae-Mensah I. Synthetic and Naturally Occurring Heterocyclic Anticancer Compounds with Multiple Biological Targets. *Molecules*. 2021;26(23):7134.
71. Jebir MR, Mustafa YF. Kidney stones: natural remedies and lifestyle modifications to alleviate their burden. *International Urology and Nephrology*. 2024;56(3):1025–33.
72. Rammohan A, Venkatesh BC, Basha NM, Zyryanov G V., Nageswararao M. Comprehensive review on natural pharmacophore tethered 1,2,3-triazoles as active pharmaceuticals. *Chemical Biology & Drug Design*. 2023;101(5):1181–203.
73. Subramani Karthikeyan Maria Grishina SKRMARSCGNP, Kennedy LJ. A review on medicinally important heterocyclic compounds and importance of biophysical approach of underlying the insight mechanism in biological environment. *Journal of Biomolecular Structure and Dynamics*. 2023;41(23):14599–619.
74. Kabir E, Uzzaman M. A review on biological and medicinal impact of heterocyclic compounds. *Results in Chemistry*. 2022;4:100606.
75. Zeki NM, Mustafa YF. 6,7-Coumarin-heterocyclic hybrids: A comprehensive review of their natural sources, synthetic approaches, and bioactivity. *Journal of Molecular Structure*. 2024;1303:137601.
76. Reddy DS, Kongot M, Kumar A. Coumarin hybrid derivatives as promising leads to treat tuberculosis: Recent developments and critical aspects of structural design to exhibit anti-tubercular activity. *Tuberculosis*. 2021;127:102050.
77. Chen C, Tang ZB, Liu Z. Recent advances in the synthesis and applications of furocoumarin derivatives. *Chinese Chemical Letters*. 2023;34(9):108396.
78. Almalki FA. An overview of structure-based activity outcomes of pyran derivatives against Alzheimer's disease. *Saudi Pharmaceutical Journal*. 2023;31(6):998–1018.
79. Rafiee F, Hasani S. Exciting progress in the transition metal-catalyzed synthesis of oxepines, benzoxepines, dibenzoxepines, and other derivatives. *Applied Organometallic Chemistry*. 2022;36(3).
80. Malamati – Konstantina K, Dimitra HL. Coumarin derivatives as therapeutic candidates: a review of their updated patents (2017–present). *Expert Opinion on Therapeutic Patents*. 2024;34(12):1231–54.
81. Jasim SF, Mustafa YF. Synthesis and Antidiabetic Assessment of New Coumarin-Disubstituted Benzene Conjugates: An In Silico-In Virto Study. *Journal of Medicinal and Chemical Sciences*. 2022;5(6):887–99.
82. Waheed SA, Mustafa YF. Novel naphthalene-derived coumarin composites: synthesis, antibacterial, and antifungal activity assessments. *Eurasian Chemical Communications*. 2022;4(8):709–24.
83. Zeki NM, Mustafa YF. Annulated Heterocyclic[g]Coumarin Composites: Synthetic Approaches and Bioactive Profiling. *Chemistry and Biodiversity*. 2024;21(3):e202301855.
84. Jibroo RN, Mustafa YF, Al-Shakarchi W. Synthesis and evaluation of linearly fused thiadiazolocoumarins as prospects with broad-spectrum bioactivity. *Results in Chemistry*. 2024;7:101494.
85. Waheed SA, Mustafa YF. Benzocoumarin backbone is a multifunctional and affordable scaffold with a vast scope of biological activities. *Journal of Medicinal and Chemical Sciences*. 2022;5(5):703–21.
86. Dorababu A. Pharmacological report of recently designed multifunctional coumarin and coumarin–heterocycle derivatives. *Archiv der Pharmazie*. 2022;355(2):e2100345.
87. Sharifi-Rad J, Ozleyen A, Boyunegmez Tumer T, Oluwaseun Adetunji C, El Omari N, Balahbib A, Taheri Y, Bouyahya A, Martorell M, Martins N, C. Cho W. Natural Products and Synthetic Analogs as a Source of Antitumor Drugs. *Biomolecules*. 2019;9(11):679.
88. Amabile C, Abate T, Chianese S, Musmarra D, Muñoz R. Exploring 1,3-Dioxolane Extraction of Poly(3-hydroxybutyrate) and Poly(3-hydroxybutyrate-co-3-hydroxyvalerate) from *Methylocystis hirsuta* and Mixed Methanotrophic Strain: Effect of Biomass-to-Solvent Ratio and Extraction Time. *Polymers*. 2024;16(13):1910.
89. Podgorski D, Krabbe S, Le L, Sierszulski P, Mohan R. Bismuth Compounds in Organic Synthesis: Synthesis of Dioxanes, Dioxepines, and Dioxolanes Catalyzed by Bismuth(III) Triflate. *Synthesis*. 2010;2010(16):2771–5.
90. Min LJ, Wang H, Bajsa-Hirschel J, Yu CS, Wang B, Yao MM, Han L, Cantrell CL, Duke SO, Sun NB, Liu XH. Novel Dioxolane Ring Compounds for the Management of Phytopathogen Diseases as Ergosterol Biosynthesis Inhibitors: Synthesis, Biological Activities, and Molecular Docking. *Journal of Agricultural and Food Chemistry*. 2022;70(14):4303–15.
91. Ferrié L. Advances in the synthesis of 1,2-dioxolanes and 1,2-dioxanes. *Advances in Heterocyclic Chemistry*. 2021;135:57–146.

92. Bohman B, Tröger A, Franke S, Lorenzo MG, Francke W, Unelius CR. Structure Elucidation and Synthesis of Dioxolanes Emitted by Two Triatoma Species (Hemiptera: Reduviidae). *Journal of Natural Products*. 2011;74(4):690–4.
93. Dhandabani GK, Jeyakannu P, Shih CL, Abraham AM, Senadi GC, Wang JJ. A Regioselective [3 + 2] Cycloaddition of Alkynols and Ketones To Access Diverse 1,3-Dioxolane Scaffolds. *The Journal of Organic Chemistry*. 2024;89(1):719–24.
94. Franchini S, Battisti UM, Sorbi C, Tait A, Cornia A, Jeong LS, Lee SK, Song J, Loddo R, Madeddu S, Sanna G, Brasili L. Synthesis, structural characterization and biological evaluation of 4'-C-methyl- and phenyl-dioxolane pyrimidine and purine nucleosides. *Archives of Pharmacological Research*. 2017;40:537–49.
95. Hellmuth M, Chen B, Bariki C, Cai L, Cameron F, Wildenberg A, Huang C, Faller S, Ren Y, Beeckmann J, Leonhard K, Heufer KA, Hansen N, Pitsch H. A Comparative Study on the Combustion Chemistry of Two Bio-hybrid Fuels: 1,3-Dioxane and 1,3-Dioxolane. *The Journal of Physical Chemistry A*. 2023;127(1):286–99.
96. Kahtan Bashir M, Abdul-Wahhab Al-Omari N, Othman Omar A. Synthesis and Evaluation of New Series of 1,3-Dioxolane Conjugated with Coumarin-Pyrazoline Derivatives as Anticancer Agents. *International Journal of Enhanced Research in Science*. 2018;7(6):2319–7463.
97. Patra I, Ansari MJ, Saadon N, Mashhadani ZI Al, Obaid NH, Alawsi T, Jabbar AH, Mustafa YF. Insights into the Electronic Properties of Coumarins: A Comparative Study Photocatalytic Degradation of Methylene Blue. *Physical Chemistry Research*. 2023;11(2):437–47.
98. Mustafa YF. Combretastatin A4-based coumarins: synthesis, anticancer, oxidative stress-relieving, anti-inflammatory, biosafety, and in silico analysis. *Chemical Papers*. 2024;78:3705–3720.
99. Waheed SA, Mustafa YF. Synthesis and evaluation of new coumarins as antitumor and antioxidant applicants. *Journal of Medicinal and Chemical Sciences*. 2022;5(5):808–19.
100. Mustafa YF. 3-mercaptocoumarins as potential bioactive candidates: From novel synthesis to comparative analysis. *Journal of Molecular Structure*. 2025;1320:139657.
101. Jasim SF, Mustafa YF. New fused-coumarin composites: Synthesis, anticancer and antioxidant potentials evaluation. *Eurasian Chemical Communications*. 2022;4(7):607–19.
102. Mustafa YF, Ismael RN, Jebir RM. Natural coumarins from two cultivars of watermelon seeds as biosafe anticancer agents, an algorithm for their isolation and evaluation. *Journal of Molecular Structure*. 2024;1295(P1):136644.
103. Younes AH, Mustafa YF. Unveiling the Biomedical Applications of Novel Coumarins Isolated From Capsicum Annuum L. Seeds by a Multivariate Extraction Technique. *Chemistry and Biodiversity*. 2024;21(6):e202400581.
104. Zeki NM, Mustafa YF. Synthesis of Novel Dioxathiole-6,7-coumarin Hybrids As Cytosafe-Multifunctional Applicants: An In Vitro—In Silico Study. *Russian Journal of Bioorganic Chemistry*. 2024;50(5):2076–91.
105. Khalil RR, Mohammed ET, Mustafa YF. Evaluation of in vitro antioxidant and antidiabetic properties of *Cydonia Oblonga* seeds' extracts. *Journal of Medicinal and Chemical Sciences*. 2022;5(6):1048–58.
106. Waheed SA, Mustafa YF. The in vitro effects of new albocarbon-based coumarins on blood glucose-controlling enzymes. *Journal of Medicinal and Chemical Sciences*. 2022;5(6):954–67.
107. Mustafa YF. Synthesis, characterization and antibacterial activity of novel heterocycle, coumacine, and two of its derivatives. *Saudi pharmaceutical journal*. 2018;26(6):870–5.
108. Jebir RM, Mustafa YF. Novel coumarins isolated from the seeds of *Citrullus lanatus* as potential antimicrobial agents. *Eurasian Chemical Communications*. 2022;4(8):692–708.
109. Jebir RM, Mustafa YF. Natural Products Catalog of Allsweet Watermelon Seeds and Evaluation of Their Novel Coumarins as Antimicrobial Candidates. *Journal of Medicinal and Chemical Sciences*. 2022;5(5):831–47.
110. Mustafa YF. 4-Chloroskimmetine-based derivatives as potential anticancer and antibacterial prospects: Their synthesis and in vitro inspections. *Results in Chemistry*. 2024;7:101511.
111. Mustafa YF. Synthesis of 7,8-dihydroxy-4-phenylbenzo[g]coumarins as potential multitarget anti-skin-aging candidates. *Journal of Molecular Structure*. 2025;1321:139806.
112. Zeki MN, Mustafa YF. Synthesis and evaluation of novel ring-conjugated coumarins as biosafe broad-spectrum antimicrobial candidates. *Journal of Molecular Structure*. 2024;1309:138192.
113. Mustafa YF. Synthesis of novel 6-aminocoumarin derivatives as potential –biocompatible antimicrobial and anticancer agents. *Journal of Molecular Structure*. 2025;1320:139658.
114. Oglah MK, Kahtan Bashir M, Mustafa YF, Mohammed ET, Khalil RR. Synthesis and biological activities of 3,5-disubstituted-4-hydroxycinnamic acids linked to a functionalized coumarin. *Systematic Review Pharmacy*. 2020;11(6):717–25.
115. Zeki NM, Mustafa YF. Novel heterocyclic coumarin annulates: synthesis and figuring their roles in biomedicine, bench-to-bedside investigation. *Chemical Papers*. 2024;78:4935–51.
116. Yang J, Luo J, Tian X, Zhao Y, Li Y, Wu X. Progress in Understanding Oxidative Stress, Aging, and Aging-Related Diseases. *Antioxidants*. 2024;13(4):394.
117. Mustafa YF. Harmful Free Radicals in Aging: A Narrative Review of Their Detrimental Effects on Health. *Indian Journal of Clinical Biochemistry*. 2024;39(2):154–67.

118. Mustafa YF, Faisal AF, Alshaher MM, Hassan DA. Food-Derived Micronutrients as Alleviators of Age-Related Dysfunction: A Dive into Their Effects and Cellular Mechanisms. *Indian Journal of Clinical Biochemistry*. 2025; <https://doi.org/10.1007/s12291-024-01297-7>
119. Mustafa YF. Coumarins from carcinogenic phenol: synthesis, characterization, in silico, biosafety, anticancer, antioxidant, and anti-inflammatory assessments. *Chemical Papers*. 2024;78:493–504.
120. Bai Y, Yang W, Jia R, Sun J, Shen D, Liu H, Yuan S. The recent advance and prospect of poly(ADP-ribose) polymerase inhibitors for the treatment of cancer. *Medicinal Research Reviews*. 2025;45(1):214–73.
121. Farhat J, Alzyoud L, Alwahsh M, Al-Omari B. Structure–Activity Relationship of Benzofuran Derivatives with Potential Anticancer Activity. *Cancers*. 2022;14(9):2196.
122. Abdulaziz NT, Mustafa YF. Antibacterial and Antitumor Potentials of Some Novel Coumarins. *International Journal of Drug Delivery Technology*. 2022;12(1):239–47.
123. Sadiq SC, Joy MP, Aiswarya SU, Ajmani A, Keerthana CK, Rayginia TP, Isakov N, Anto RJ. Unlocking nature’s pharmacy: an in-depth exploration of phytochemicals as potential sources of anti-cancer and anti-inflammatory molecules. *Exploration of Drug Science*. 2024;2(6):744–84.
124. Mustafa YF. Biocompatible new coumarins as dual-target anti-inflammatory agents: Insights from chemistry to toxicity. *Next Research*. 2025;2(2):100236.
125. Sharma S, Kumar D, Singh G, Monga V, Kumar B. Recent advancements in the development of heterocyclic anti-inflammatory agents. *European Journal of Medicinal Chemistry*. 2020;200:112438.
126. Barangi VC, Shastri LA, Chowdegowda PK, Sangappanavar R, Inamdar K, Dalbanjan NP, Barretto DA, Sunagar V. Design and synthesis of new coumarin-1,2,3-triazole hybrids as new antidiabetic agents: In vitro α -amylase, α -glucosidase inhibition, anti-inflammatory, and docking study. *European Journal of Chemistry*. 2024;15(3):205–19.
127. Abdelaziz E, El-Deeb NM, Zayed MF, Hasanein AM, El Sayed IET, Elmongy EI, Kamoun EA. Synthesis and in-vitro anti-proliferative with antimicrobial activity of new coumarin containing heterocycles hybrids. *Scientific Reports*. 2023;13(1).
128. Varghese M, Balachandran M. Antibacterial efficiency of carbon dots against Gram-positive and Gram-negative bacteria: A review. *Journal of Environmental Chemical Engineering*. 2021;9(6):106821.
129. Mustafa YF. Coumarins from toxic phenol: An algorithm of their synthesis and assessment as biosafe, wide-spectrum, potent antimicrobial prospects. *Applied Chemical Engineering*. 2024;7(3):5527.
130. Elsebaei MM, Ezzat HG, Helal AM, El-Shershaby MH, Abdulrahman MS, Alsedawy M, Aljohani AKB, Almaghribi M, Alsulaimany M, Almohaywi B, Alghamdi R, Miski SF, Musa A, Ahmed HEA. Rational design and synthesis of novel phenyltriazole derivatives targeting MRSA cell wall biosynthesis. *RSC Advances*. 2024;14(54):39977–94.
131. Shinada NK, de Brevern AG, Schmidtke P. Halogens in protein–ligand binding mechanism: A structural perspective. *Journal of Medicinal Chemistry*. 2019;62(21):9341–56.
132. Abdelaziz SA, Ahmed EM, Sadek M. Preparation Of Novel Multihydrophilic Anionic-Nonionic Sugar-Based Surfactants: I-Study Of Surface Activity, Performance, Detergency And Antimicrobial Assessment. *Egyptian Journal of Chemistry*. 2024;0–0.
133. Mustafa YF. New Coumarin-Metronidazole Composites: Synthesis, Biocompatibility, and Anti-anaerobic Bacterial Activity. *Russian Journal of Bioorganic Chemistry*. 2024;50(1):201–10.
134. Jasim SF, Mustafa YF. Synthesis, ADME Study, and antimicrobial evaluation of novel naphthalene-based derivatives. *Journal of Medicinal and Chemical Sciences*. 2022;5(5):793–807.
135. Ferreira AR, Alves D da N, de Castro RD, Perez-Castillo Y, de Sousa DP. Synthesis of Coumarin and Homoisoflavonoid Derivatives and Analogs: The Search for New Antifungal Agents. *Pharmaceuticals*. 2022;15(6):712.
136. Mahmood AT, Kamal IK, Mustafa YF. Coumarin Backbone as a Door-Opening Key for Investigating Chloroxynolol as Oral Antimicrobial Agents: an In Vitro–In Silico Study. *Russian Journal of Bioorganic Chemistry*. 2024;50(6):2252–68.
137. Mousa S, Sarfraz M, Mousa WK. The Interplay between Gut Microbiota and Oral Medications and Its Impact on Advancing Precision Medicine. *Metabolites*. 2023;13(5):674.
138. Mustafa YF, Zain Al-Abdeen SH, Khalil RR, Mohammed ET. Novel functionalized phenyl acetate derivatives of benzo [e]-bispyrone fused hybrids: Synthesis and biological activities. *Results in Chemistry*. 2023;5:100942.
139. Kamal IK, Mahmood AT, Mustafa YF. Synthesis of Eugenol-Derived Coumarins as Broad-Spectrum Biosafe Antimicrobial Agents. *Russian Journal of Bioorganic Chemistry*. 2024;50(6):2240–51.
140. Mustafa YF. Triple coumarin-based 5-fluorouracil prodrugs, their synthesis, characterization, and release kinetics. *Journal of Molecular Structure*. 2024;1301:137415.
141. Campos KR, Coleman PJ, Alvarez JC, Dreher SD, Garbaccio RM, Terrett NK, Tillyer RD, Truppo MD, Parmee ER. The importance of synthetic chemistry in the pharmaceutical industry. *Science*. 2019;363(6424).
142. Pawar B, Behera SK, Tekade M, Al-Shar’i N, Tekade RK. Computer-aided technologies in drug discovery and toxicity prediction. In: *Essentials of Pharmacotoxicology in Drug Research, Volume 1 Elsevier*; 2023. p. 239–54.
143. Al-Shakarchi W, Saber Y, Merkhan MM, Mustafa YF. Sub Chronic Toxicity Study of Coumacines. *Pharmacognosy Journal*. 2023;15(1):160–4.

144. Hemmerich J, Ecker GF. In silico toxicology: From structure–activity relationships towards deep learning and adverse outcome pathways. *WIREs Computational Molecular Science*. 2020;10(4).
145. Mustafa YF, Bashir MK, Oglah MK. Influence of albobcarbon-cyclic hybridization on biomedical activities: A review. *Journal of Medicinal and Chemical Sciences*. 2022;5(4):518–35.
146. Sindhuja S, Karnan M, Gayathri R, Kavimani M. Non-covalent interaction, topology, molecular properties, spectral and quantum chemical analysis of 2,5-dinitrophenol. *Journal of the Indian Chemical Society*. 2024;101(10):101276.
147. Fernandes F, Dias-Teixeira M, Delerue-Matos C, Grosso C. Critical Review of Lipid-Based Nanoparticles as Carriers of Neuroprotective Drugs and Extracts. *Nanomaterials*. 2021;11(3):563.
148. Kasim SM, Abdulaziz NT, Jasim MH, Mustafa YF. Resveratrol in cancer chemotherapy: Is it a preventer, protector, or fighter? *Eurasian Chemical Communications*. 2023;5(7):576–87.
149. Marques L, Costa B, Pereira M, Silva A, Santos J, Saldanha L, Silva I, Magalhães P, Schmidt S, Vale N. Advancing Precision Medicine: A Review of Innovative In Silico Approaches for Drug Development, Clinical Pharmacology and Personalized Healthcare. *Pharmaceutics*. 2024;16(3):332.
150. Gonçalves JE. Challenges Faced in the Development of Computational Methods for Predicting Pharmacokinetics Behavior. In 2024. p. 385–99.
151. Zeki NM, Mustafa YF. Coumarin hybrids for targeted therapies: A promising approach for potential drug candidates. *Phytochemistry Letters*. 2024;60:117–33.
152. Shah P, Jogani V, Bagchi T, Misra A. Role of Caco-2 Cell Monolayers in Prediction of Intestinal Drug Absorption. *Biotechnology Progress*. 2006;22(1):186–98.
153. Elbahnsi A, Dudas B, Cisternino S, Declèves X, Miteva MA. Mechanistic insights into P-glycoprotein ligand transport and inhibition revealed by enhanced molecular dynamics simulations. *Computational and Structural Biotechnology Journal*. 2024;23:2548–64.
154. Zeki NM, Mustafa YF. Digital alchemy: Exploring the pharmacokinetic and toxicity profiles of selected coumarin-heterocycle hybrids. *Results in Chemistry*. 2024;10:101754.
155. Zhao M, Ma J, Li M, Zhang Y, Jiang B, Zhao X, Huai C, Shen L, Zhang N, He L, Qin S. Cytochrome P450 Enzymes and Drug Metabolism in Humans. *International Journal of Molecular Sciences*. 2021;22(23):12808.
156. Mohammed Alshaher M, Fakri Mustafa Y. From laboratory to computer models: Enhancing coumarin discovery through interdisciplinary research. *Applied Chemical Engineering*. 2025;8(1):5613.
157. Talevi A, Bellera CL. Drug Binding to Plasma Proteins. In: *The ADME Encyclopedia Cham: Springer International Publishing*; 2022. p. 315–26.
158. Vatansever S, Schlessinger A, Wacker D, Kaniskan HÜ, Jin J, Zhou M, Zhang B. Artificial intelligence and machine learning-aided drug discovery in central nervous system diseases: State-of-the-arts and future directions. *Medicinal Research Reviews*. 2021;41(3):1427–73.
159. Usman M, Alam A, Zainab, Khan M, Elhenawy AA, Ayaz M, Alanazi MM, Latif A, Shah SAA, Ali M, Ahmad M. Synthesis, characterization, enzyme inhibition and molecular docking studies of benzothiazole derivatives bearing alkyl phenyl ether fragments. *Journal of Molecular Structure*. 2025;1319:139504.